Original Research Article

Virulence of *Agrobacterium tumefaciens* requires Lipid Homeostasis mediated by the Lysyl-Phosphatidylglycerol Hydrolase AcvB

Maike K. Groenewold[1,a], Stefanie Hebecker[2,a], Christiane Fritz[3], Simon Czolkoss[3], Milan Wiesselmann[2], Dirk W. Heinz[1], Dieter Jahn[2], Franz Narberhaus[3], Meriyem Aktas[3,b] and Jürgen Moser[2,b]

[1]Structure and Function of Proteins, Helmholtz Centre for Infection Research, 38124 Braunschweig, Germany.
[2]Institute for Microbiology, Technische Universität Braunschweig, 38106 Braunschweig, Germany.
[3]Lehrstuhl für Biologie der Mikroorganismen, Ruhr-Universität Bochum, 44780 Bochum, Germany.
[a]M.G. and S.H. contributed equally to this work.
[b]M.A. and J.M. should be considered joined senior author.

Correspondence: Jürgen Moser (j.moser@tu-bs.de), phone: +49 531 3915808

RUNNING TITLE: L-PG hydrolysis by AcvB

KEYWORDS: *Agrobacterium tumefaciens*, lysyl-phosphatidylglycerol, lipid homeostasis, virulence, type IV secretion

ACKNOWLEDGMENTS

We thank Simone Virus for technical assistance and Prof Ute Krämer for proving the phytochamber. This work was supported by the Deutsche Forschungsgemeinschaft: MO 1749/1-2, HE 1852/14-2 and Research Training Group GRK 2341 (Microbial Substrate Conversion (MiCon).

SUMMARY

Agrobacterium tumefaciens transfers oncogenic T-DNA via the type IV secretion system (T4SS) into plants causing tumor formation. The *acvB* gene encodes a virulence factor of unknown function required for plant transformation. Here we specify AcvB as a periplasmic lysyl-phosphatidylglycerol (L-PG) hydrolase, which modulates L-PG homeostasis. Via functional characterization of recombinant AcvB variants, we showed that the C-terminal domain of AcvB (residues 232–456) is sufficient for full enzymatic activity and defined key residues for catalysis. Absence of the hydrolase resulted in ~10-fold increase of L-PG in *Agrobacterium* membranes and abolished T-DNA transfer and tumor formation. Overproduction of the L-PG synthase gene (*lpiA*) in wild type *A. tumefaciens* resulted in a similar increase of the L-PG content (~7-fold) and a virulence defect even in the presence of intact AcvB. These results suggest that elevated L-PG amounts (either by overproduction of the synthase or absence of the hydrolase) are responsible for the virulence phenotype. Gradually increasing the L-PG content by complementation with different *acvB* variants revealed that cellular L-PG levels above 3% of total phospholipids interfere with T-DNA transfer. Cumulatively, this study identified AcvB as a novel virulence factor required for membrane-lipid homeostasis and T-DNA transfer.

INTRODUCTION

The Gram-negative soil bacterium *Agrobacterium tumefaciens* infects dicotylic plant species and causes crown gall disease by the transfer and integration of oncogenic transfer DNA (T-DNA) into the plant genome (Hooykaas & Beijersbergen, 1994). The tumor inducing (Ti) plasmid harbors multiple virulence (*vir*) genes, which facilitate the translocation of the single stranded T-DNA together with further effector molecules. Induction of *vir* gene expression is mediated by extracellular acidity, phenolic compounds and monosaccharides from wounded plant cells. VirA acts as a sensor kinase that phosphorylates VirG. Activated VirG proteins turn on transcription of genes for the type IV secretion system (T4SS), which then facilitates T-DNA transfer (Winans, 1992, Christie, 2004). The T4SS is mainly composed of proteins VirB1-VirB11 and VirD4,

which are arranged as a huge super complex spanning both the inner and outer bacterial membrane. The apparatus is energized by the ATPases VirD4, VirB4 and VirB11. Components VirB6 – VirB10 form the scaffold of the translocation channel and proteins VirB2, VirB5 and VirB7 assemble the needle-like structure that extends the extracellular surface of *A. tumefaciens* for T-DNA and effector protein transport (Chandran Darbari & Waksman, 2015, Christie & Cascales, 2005, Grohmann *et al.*, 2018, Wallden *et al.*, 2010). Integration and expression of the T-DNA encoded oncogenes results in the biosynthesis of phytohormones, which induce enhanced proliferation of plant cells resulting crown gall formation (Morris, 1986).

In early investigations, the chromosomally localized *acvB* gene (*Agrobacterium* chromosomal virulence protein B) and the Ti-plasmid encoded *virJ* gene were identified as T4SS related virulence factors. *A. tumefaciens* strains with the nopaline-type Ti-plasmid (pTiC58) solely contain *acvB* (e.g. strain C58). By contrast, strains harboring the octopine-type Ti-plasmid (pTiA6) additionally possess the plasmid-localized *virJ* gene (Kalogeraki & Winans, 1995, Pan *et al.*, 1995, Wirawan *et al.*, 1993). The protein sequence of VirJ shows a high degree of sequence conservation to the C-terminal half of AcvB. Expression of *virJ* is controlled by the VirA/VirG two-component system via stimulation with phenolic compounds, whereas expression of *acvB* is independent of this system (Kalogeraki & Winans, 1995, Pan *et al.*, 1995). Functional similarity of AcvB and VirJ was indicated by the successful complementation of an *acvB* mutant with *virJ* (Kalogeraki & Winans, 1995). The *acvB* mutant strain showed no defect with respect to plant cell attachment and T-strand formation but was attenuated in T-DNA transfer to the host cell (Pan *et al.*, 1995). Several postulated activities of AcvB/VirJ have been discussed. First, T-strand binding (possibly via effector proteins) of AcvB and VirJ to mediate its transfer to plant cells was shown (Gede Putu Wirawan & Kojima, 1996, Kalogeraki & Winans, 1995, Kang *et al.*, 1994, Pantoja *et al.*, 2002). However, T-strand interaction of AcvB and VirJ was challenged in a subsequent investigation (Cascales & Christie, 2004). Alternatively, a possible function as periplasmic chaperone was proposed (Cascales & Christie, 2003, Atmakuri *et al.*, 2003). Overall, the actual molecular function(s) of AcvB or VirJ have remained elusive.

In *A. tumefaciens* C58, the *acvB* gene is localized on the circular chromosome in tandem downstream of the *lpiA* gene (low pH inducible protein A) (Fig. 1A) (Vinuesa *et al.*, 2003). The *lpiA* gene encodes an aminoacyl-phosphatidylglycerol synthase, which is strictly specific for the synthesis of lysyl-phosphatidylglycerol (L-PG) when expressed in *E. coli* (Roy & Ibba, 2009), whereas orthologous enzymes facilitate the synthesis of alanyl-PG (A-PG) using the

corresponding A-PG synthase (A-PGS) or display a broad substrate specificity (Fields & Roy, 2017). Amino acids for these reactions are provided by aminoacyl-tRNAs (Fields & Roy, 2017, Roy, 2009). Our laboratory contributed to the molecular understanding of the A-PGS system from the human pathogen *Pseudomonas aeruginosa* (Klein *et al.*, 2009, Hebecker *et al.*, 2011, Hebecker *et al.*, 2015). Furthermore, we characterized a related A-PG hydrolase (A-PGH), which is encoded in an operon with A-PGS (Arendt *et al.*, 2013). In concert, this A-PGS/A-PGH system balances the cellular A-PG concentration (Arendt *et al.*, 2013), which is essential for the antimicrobial susceptibility of *P. aeruginosa* (Arendt *et al.*, 2012).

Based on genome comparisons, the presence of an orthologous aminoacyl-PGS/-PGH pair was postulated in *A. tumefaciens* (Arendt et al., 2013). In the present investigation, we elucidated the molecular functions of AcvB and LpiA. Our results explain the long-described phenotype of the avirulent *acvB* deletion strain.

RESULTS

Genes for LpiA and AcvB are encoded in an operon

Genome comparisons indicated an operon structure for *lpiA* and *acvB* genes in various Gram-negative organisms (Arendt *et al.*, 2013, Vinuesa *et al.*, 2003). *A. tumefaciens* LpiA was shown to synthesize L-PG (Roy & Ibba, 2009), whereas a lipase activity was postulated for AcvB (Fig. 1A). *A. tumefaciens* AcvB has 32% sequence identity with the recently described A-PGH from *P. aeruginosa*. Furthermore, a typical lipase signature Gly-X-Ser-X-Gly (Sigrist *et al.*, 2013) containing a potential active site serine residue (Ser-336) was identified. This specific motif together with two additional sequence regions comprising fully conserved serine and histidine residues (Ser-269 and His-433) (Fig. 1B) suggest that *A. tumefaciens* AcvB might have aminoacyl-PG hydrolase activity. Accordingly, an involvement of the virulence factor in the DNA transfer machinery was questioned and a functional role of AcvB in lipid homeostasis was explored on the basis of biochemical analyses and plant-infection experiments.

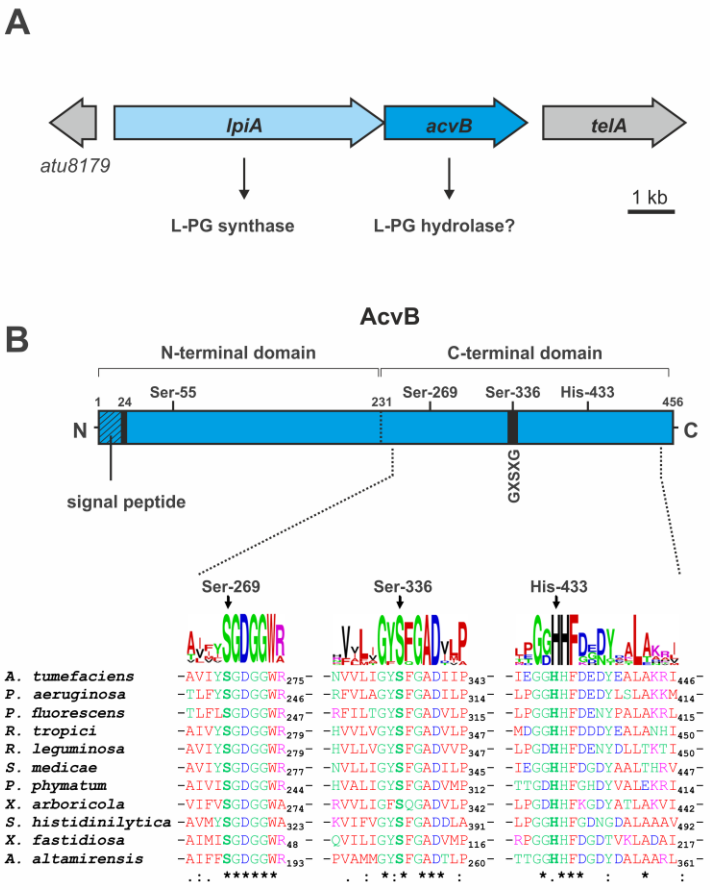

Fig. 1: Genetic organization of *acvB* in *A. tumefaciens* and proposed enzymatic activity of the gene products. (A) The *acvB* gene is organized in a putative operon with *lpiA* on the circular chromosome. (B) Postulated domain structure of AcvB and partial sequence alignment of orthologous AcvB proteins. Gene names are given as follows. *Agrobacterium tumefaciens* (or *Agrobacterium fabrum* str. C58), AAK88253.1; *Pseudomonas aeruginosa* PAO1, AAG04308.1; *Pseudomonas fluorescens*, AUM68555.1; *Rhizobium tropici* CIAT 899, AAN52238.1; *Rhizobium leguminosarum*, ANP87087.1; *Sinorhizobium medicae* WSM419, AAP21142.1; *Paraburkholderia phymatum*, WP_012403314.1; *Xanthomonas arboricola* pv. *fragariae*, SOU12047.1; *Sphingomonas histidinilytica*, SKB26083.1; *Xylella fastidiosa*, AAF83564.1; *Aureimonas altamirensis*, KHJ55928.1. The conservation pattern of three distinct regions is indicated as a sequence logo, conserved and partly conserved residues are marked by asterisk and colon or period. Amino acid positions subjected to site-directed mutagenesis are highlighted.

AcvB is composed of two paralogous protein domains

Sequence analyses suggest a two-domain architecture for AcvB. The N-terminal half (amino acids 1-231) shows 21% sequence identity to the C-terminal half (amino acid 232-456) which might indicate that both domains have evolved from a predecessor by gene duplicationThe key conserved residues (Ser-269, Ser-336, His-433, Fig. 1B) are located in the C-terminal domain of AcvB and only Ser-269 possesses a direct counterpart in the N-terminal domain (Ser-55). This might indicate that the C-terminal domain harbors essential residues for the proposed lipase activity of AcvB. To test this assumption, an N-terminally truncated protein variant, which is devoid of amino acid residues 1–231 ($AcvB_{232\text{-}456}$) was included in our functional analysis.

AcvB is a soluble periplasmic protein

Bioinformatic predictions (Nielsen, 2017) suggest a N-terminal signal sequence for the periplasmic localization of AcvB with a potential cleavage site after amino acid 24. The cellular localization of AcvB was experimentally elucidated using a translational fusion of AcvB with PhoA. Translated PhoA shows enzymatic activity only after translocation to the periplasm (Hoffman & Wright, 1985). Alkaline phosphatase activity was analysed from whole cells or alternatively after subcellular fractionation. Plasmids encoding PhoA with its native leader (positive control, native-PhoA), PhoA without signal sequence (negative control, Δss-PhoA) and a fusion of the 24 N-terminal residues of AcvB with PhoA (AcvB-PhoA) were introduced into *A. tumefaciens.* AcvB-PhoA was secreted into the periplasm, as indicated by the conversion of the PhoA-specific substrate (BCIP) and the resulting blue color of the related colonies (compare

AcvB-PhoA with Δss-PhoA and native–PhoA) (Fig. 2A). Obviously, the N-terminal signal sequence region of AcvB is sufficient to direct the heterologous PhoA-fusion protein to the periplasm. Next, we checked whether AvcB is soluble or anchored to the inner membrane similar to *P. aeruginosa* A-PGH, which is attached to the outer surface of the inner membrane via its non-cleaved N-terminal signal sequence (Arendt et al., 2013). The phosphatase activity of the periplasmic and cytoplasmic fractions of all three strains was measured as outlined in Material and Methods. In parallel and as control, the endogenous activity of the cytoplasm-localized malate dehydrogenase was monitored to quantify potential cross contamination of periplasmic fractions (de Maagd & Lugtenberg, 1986). Only minor malate dehydrogenase activities ranging from 0.1 – 0.3% relative to the overall cellular malate dehydrogenase activity were observed in all tested periplasmic fractions. PhoA-mediated alkaline phosphatase activity of AcvB-PhoA in the periplasm was 5.2-fold increased in comparison to Δss-PhoA (Fig. 2B). Thus, we concluded that AcvB is a soluble periplasmic protein, which is in agreement with previous immunoassay-based AcvB localization experiments (Kang *et al.*, 1994) and the results of related VirJ investigations (Kalogeraki & Winans, 1995, Pan *et al.*, 1995).

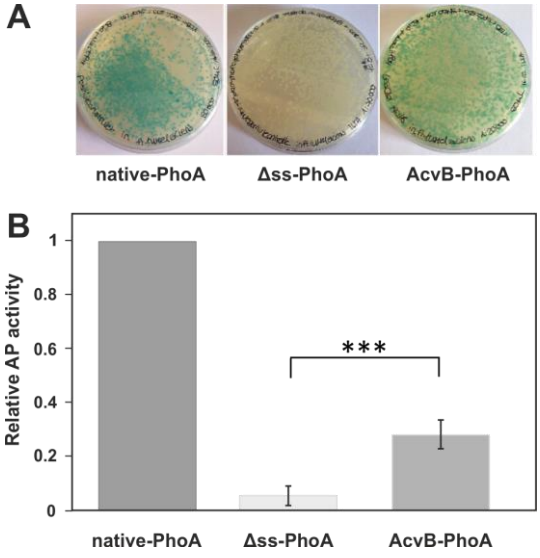

Fig. 2: Subcellular localization of AcvB. *A. tumefaciens* strains carrying plasmids encoding PhoA with its native leader (native-PhoA), PhoA without signal sequence (Δss-PhoA) and a fusion of the 24 amino terminal residues of AcvB with PhoA (AcvB-PhoA) were analysed. (A) Colonies of native-PhoA (positive control) and AcvB-PhoA are colored blue due to the conversion of the PhoA-specific substrate BCIP (compare native-PhoA and AcvB-PhoA with Δss-PhoA). (B) Periplasmic fractions were prepared from liquid cell cultures after IPTG induction by polymyxin B treatment. For all strains, alkaline phosphatase (AP) activity of the periplasmic fraction was determined. Mean values from four independent experiments are shown (*** = P<0.001).

Overproduction and purification of AcvB

For functional analysis, AcvB was overproduced in *Escherichia coli* with a N-terminal PelB leader sequence. For subsequent affinity purification from the periplasmic fraction, the protein contained a C-terminal Strep-tag-II sequence. The SDS-PAGE analysis depicted in Fig. 3 summarizes the Strep-Tactin® chromatography: A soluble periplasmic fraction (lane 1) was applied to the affinity matrix (flow-through fraction, lane 2) and after two washing steps (lanes 3 and 4) AcvB was eluted with desthiobiotin (lane 5), followed by dialysis and concentration (lane 6). A typical protein production yielded 3 mg of the purified protein from 1 l cell culture. The integrity of the mature N-terminus after signal sequence cleavage was confirmed by Edman degradation (Ala-Gln-Asp-Lys-Pro-Ala-Tyr-Glu-Thr-Gly). Analytical gel permeation chromatography (Fig. 3B) indicated a monomeric protein with a relative molecular mass of approximately 62,000 (calculated molecular weight 48,023 Da, after maturation).

For comparative biochemical investigations, an overall of five AcvB variant proteins were purified accordingly and with similar yield and purity (lanes 7 – 11 in Fig. 3A): Site-directed mutants S336A (mutation of the proposed active site serine), S269A, H433A and H433N (mutation of a highly conserved serine or histidine residue) and the N-terminally truncated variant $AcvB_{232\text{-}456}$.

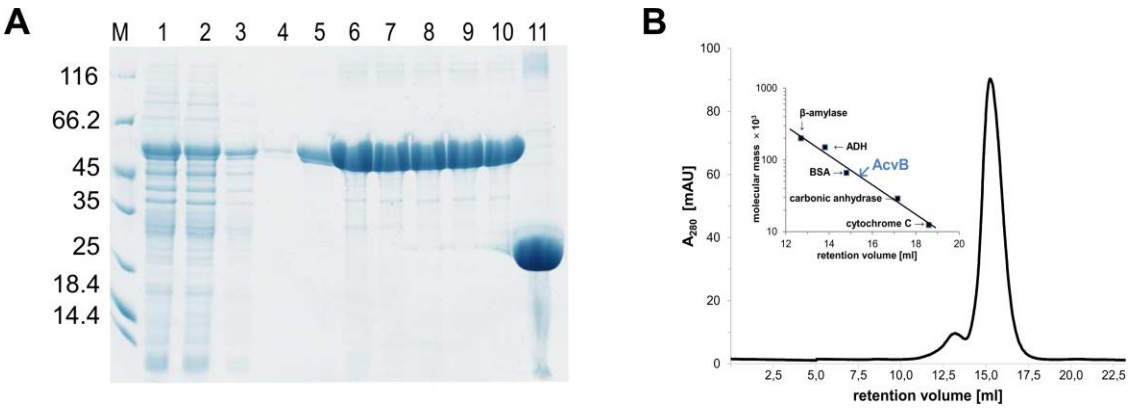

Fig. 3: Recombinant production and purification of Strep-tagged AcvB proteins and analytical gel filtration. (A) A soluble periplasmic fraction of an *E. coli* AcvB-production strain was isolated (lane 1), AcvB was affinity purified (lane 2, flow-through; lanes 3 and 4, washing steps; lane 5, desthiobiotin elution) and subsequently dialyzed and concentrated (lane 6). Mutant proteins S269A, S336A, H433A, H433N (lanes 7-10) and the N-terminally truncated variant $AcvB_{232\text{-}456}$ (lane 11) were purified and concentrated accordingly. (B) Purified AcvB (208 µM) was analysed on a Superdex 200 HR 10/30 gel permeation column at a flow rate of 0.5 ml min^{-1} by monitoring the absorbance at 280 nm on an Äkta purifier system, which was previously calibrated using protein standards β-amylase (*M*r = 200,000), alcohol dehydrogenase (ADH, *M*r = 150,000), BSA (*M*r = 66,000), carbonic anhydrase (*M*r = 29,000) and

cytochrome C (*M*r = 12,000). For recombinant AcvB, a relative molecular mass of approximately 62,000 was determined from the related calibration curve (inset).

AcvB displays esterase activity

Chromogenic nitrophenyl esters are commonly used substrates to monitor the catalytic activity of lipases and esterases. For initial *in vitro* activity analysis, we tested acetyl-*p*-nitrophenyl ester and alanyl-*p*-nitrophenyl ester as potential substrates for AcvB. The acetyl-*p*-nitrophenyl ester was not accepted by AcvB as a substrate. However, AcvB converted the amino acid derivative alanyl-*p*-nitrophenyl ester with a specific activity of 306 pmol $mg^{-1}min^{-1}$ (spontaneous substrate hydrolysis subtracted). From these experiments, it was hypothesized that the natural AcvB substrate might be an amino acid ester.

AcvB catalyzes the hydrolysis of L-PG into PG and L-lysine

Since *A. tumefaciens* LpiA is a tRNA-dependent aminoacyl-PG synthase strictly specific for L-PG formation (Reeve *et al.*, 2006, Roy, 2009), this PG derivative was investigated as a possible AcvB substrate. Enzyme activity was assayed in a micellar reaction mixture containing 2.6 µM L-PG and 1.5 mg ml^{-1} Triton™ X-100 in the presence of 10 µM purified AcvB. Two-dimensional thin layer chromatography (Fig. 4A-D) in combination with molybdatophosphoric acid (A, B) and ninhydrin (C, D) staining revealed the AcvB-dependent depletion of L-PG paralleled by the appearance of a new spot showing identical migration and staining characteristics as authentic PG (compare A, C with B, D; note that PGs are not stainable with ninhydrin). One-dimensional thin layer chromatography was used for the quantification of AcvB-dependent L-lysine release (Fig. 4E). Spot intensities were quantified by densitometry (using AlphaEase FC software) and L-lysine concentrations were calculated using an L-lysine calibration curve. A specific AcvB activity of 190 ± 3 pmol $mg^{-1}min^{-1}$ for the conversion of L-PG into L-lysine and PG was calculated (spontaneous substrate hydrolysis subtracted). These findings clearly demonstrate that the virulence factor AcvB mediates L-PG hydrolase activity.

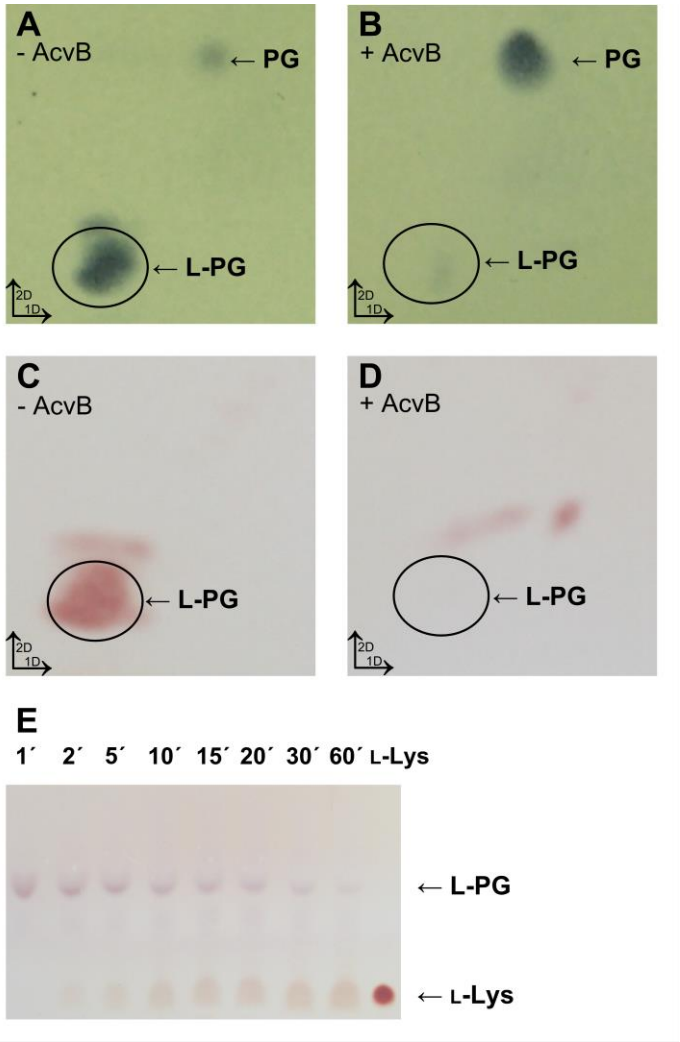

Fig. 4: *In vitro* AcvB activity assay using purified AcvB in the presence of L-PG containing micelles. (A-D) Separation of polar membrane lipids by two-dimensional thin layer chromatography and detection by molybdatophosphoric acid (A, B) and ninhydrin staining (C, D). L-PG samples always contained detectable amounts of PG due to spontaneous substrate hydrolysis. Commercial L-PG is a mixture that contains up to 15 % of an acyl migration isomer causing additional ninhydrin-positive lipid spots (E) AcvB-dependent formation of L-Lys (incubation times 0 – 60 min) from L-PG. Samples were analysed by one-dimensional thin layer chromatography and ninhydrin detection. Commercially available L-Lys was used as a reference.

In vitro activity of site-directed AcvB variants

Based on the predicted catalytic residues (Fig. 1B) and the conversion of L-PG and the artificial substrate alanyl-*p*-nitrophenyl ester, we postulated an enzymatic lipase mechanism involving catalytic serine and histidine residues. Site-directed AcvB variants were purified and the integrity of all proteins was verified by thermal stability assays (Fig. 5B). Mutant S269A showed residual activity of 11 ± 4 pmol mg^{-1} min^{-1} in the *in vitro* L-PG hydrolase assay (Fig. 5B). By contrast,

enzymatic activity was abolished when the fully conserved residues Ser-336 or His-433 were mutagenized (Fig 5B). In the S336A mutant, the proposed active site serine of the highly conserved lipase signature Gly-X-Ser-X-Gly is exchanged. Inactivity of the mutant proteins H433A and H433N suggests His-433 as a second key catalytic residue. The functional relevance of a conserved Ser/His diade was also demonstrated for the orthologous protein A-PGH of *P. aeruginosa* (Arendt *et al.*, 2013). Accordingly, a Ser-336/His-433 mediated nucleophilic mechanism for the hydrolysis of L-PGS was proposed (Fig. 5A).

The C-terminal domain of AcvB is *sufficient for L-PG hydrolysis*

The biological function(s) of proteins can often be resolved by exploring individual protein domains. AcvB theoretically comprises a two domain architecture with all key catalytic residues (Ser-269, Ser-336 and His-433) located in the C-terminal half of the protein. Therefore, the N-terminally truncated AcvB protein $AcvB_{232-456}$ with a molecular weight of 24 kDa (full length protein 48 kDa) was recombinantly produced and purified as a stable and soluble protein (Fig. 3, lane 11). The C-terminal domain was subjected to an *in vitro* activity assay in the presence of L-PG resulting in the conversion of L-PG with a specific activity of 130 ± 3 pmol $mg^{-1}min^{-1}$ (Fig. 5B). These results clearly show that the C-terminal part of AcvB contains all elements responsible for L-PG hydrolysis.

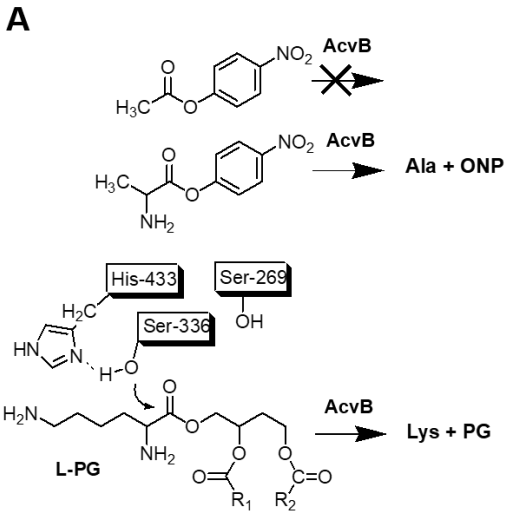

B

in vitro
L-PG hydrolysis of AcvB

AcvB variant	Activity [pmol $mg^{-1}min^{-1}$]	Tm [°C]
WT	190 ± 3	55.0
S269A	11 ± 4	54.5
S336A	n.d.	55.0
H433A	n.d.	55.0
H433N	n.d.	54.5
aa232-456	130 ± 3	-

Fig. 5: *In vitro* enzymatic activity of AcvB and variant proteins. (A) Chromogenic nitrophenyl esters (acetyl-*p*-nitrophenyl ester and alanyl-*p*-nitrophenyl ester) and L-PG were analysed as a substrate of AcvB. (B) Specific

activities of mutant AcvB proteins were determined (n.d., not detectable; detection limit 4 pmol $mg^{-1}min^{-1}$). The integrity of protein variants was confirmed in thermal shift experiments. The thermal denaturation temperature Tm of the wild-type protein and the related point mutants were determined using SYPRO Orange as a fluorophore which increases its fluorescence due to the nonspecific binding of hydrophobic surfaces (Thermofluor assay) (Niesen *et al.*, 2007). (-, not determined). Based on the sequence homology of AcvB and A-PGH (Arendt *et al.*, 2013), the artificial substrate experiments and the results of the present mutagenesis study an enzymatic mechanism for the conversion of L-PG into L-Lys and PG was proposed (A *bottom*).

The acvB mutant displays a severe growth defect under acidic conditions

To investigate the physiological relevance of L-PG homeostasis in *A. tumefaciens*, the two markerless gene-deletion mutants Δ*lpiA* and Δ*acvB* were constructed. Growth of both strains under neutral conditions (YEB medium or alternatively in AB minimal medium at pH 7.5) was equivalent to growth of the wild type strain (Fig. 6A). By contrast, growth of the *acvB* mutant was severely impaired when cultivated in acidic AB medium (AB pH 5.5). This growth defect was complemented by expression of plasmid-encoded *acvB* (Δ*acvB* (pAcvB)).

It was demonstrated that the orthologous *acvB* gene from in *Rhizobium tropici* CIAT899 is also required for acid tolerance (Vinuesa *et al.*, 2003). Furthermore, the growth phenotype of several acid-sensitive *Rhizobium meliloti* mutants was restored in the presence of calcium ions. A stabilizing effect of divalent cations on cell membranes has been well documented (Ha, 2001).

To test whether membrane integrity might be affected under acidic conditions in the *acvB* mutant, we analysed growth in acidic AB medium supplemented with 80 mM $CaCl_2$. The growth defect was partially restored by $CaCl_2$ supplementation (Fig. 6A) suggesting that deletion of a*cvB* destabilizes *Agrobacterium* membranes.

L-PG levels are drastically increased in the acvB mutant

The lipid composition of *A. tumefaciens* strains was analysed in stationary phase by two-dimensional thin layer chromatography. Densitometry (using AlphaEase FC software) after molybdatophosphoric acid staining was then used to relate the cellular L-PG content to the overall amount of (dominant) lipids (phosphatidylethanolamine (PE), phosphatidylcholine (PC), monomethyl-phosphatidylethanolamine (MMPE), PG and cardiolipin (CL)).

L-PG was barely detectable in the wild type strain grown in neutral LB and AB medium. However, *Agrobacterium* accumulated ~2% L-PG when grown under acidic conditions (Fig. 5A, AB pH 5.5) suggesting that L-PG synthesis and/or *lpiA* expression is induced by acidic pH. This

is in agreement with previously published data demonstrating that expression of both *lpiA* and *acvB* genes is upregulated under acidic conditions (Heckel *et al.*, 2014). As expected, deletion of the L-PG synthase gene *lpiA* resulted in loss of L-PG (Fig. 6B).

For strain Δ*acvB* a substantial increase of the cellular L-PG content was determined under all experimental conditions: ~3% when cultivated in YEB, ~6% when using AB pH 7.5 and ~15% in AB pH 5.5. This *in vivo* lipid accumulation confirms the L-PG hydrolase activity determined in our preceding *in vitro* experiments. When comparing culture conditions at pH 7.5 and pH 5.5, a more than 2-fold increased L-PG content indicates that strain Δ*acvB* still responds to acidic environmental conditions. Obviously, the cellular L-PG synthase activity is efficiently controlled and has a significant influence on the overall L-PG content of the (mutant) cell. For the complemented strain Δ*acvB* (p*acvB*) wild type-like lipid levels were restored.

The composition of the remaining lipids for the *lpiA*- and *acvB*-mutant strain under neutral conditions was comparable to the wild type (Fig. S1). However, under acidic growth conditions, the *acvB* mutant revealed differences with respect to the cellular concentration of PG, PC and MMPE, but only the decrease in MMPE of about 30% was consistent in all replicates (Fig. S1). This might be indicative for an indirect link between the metabolism of L-PG and the physiological adaptation to acidic conditions.

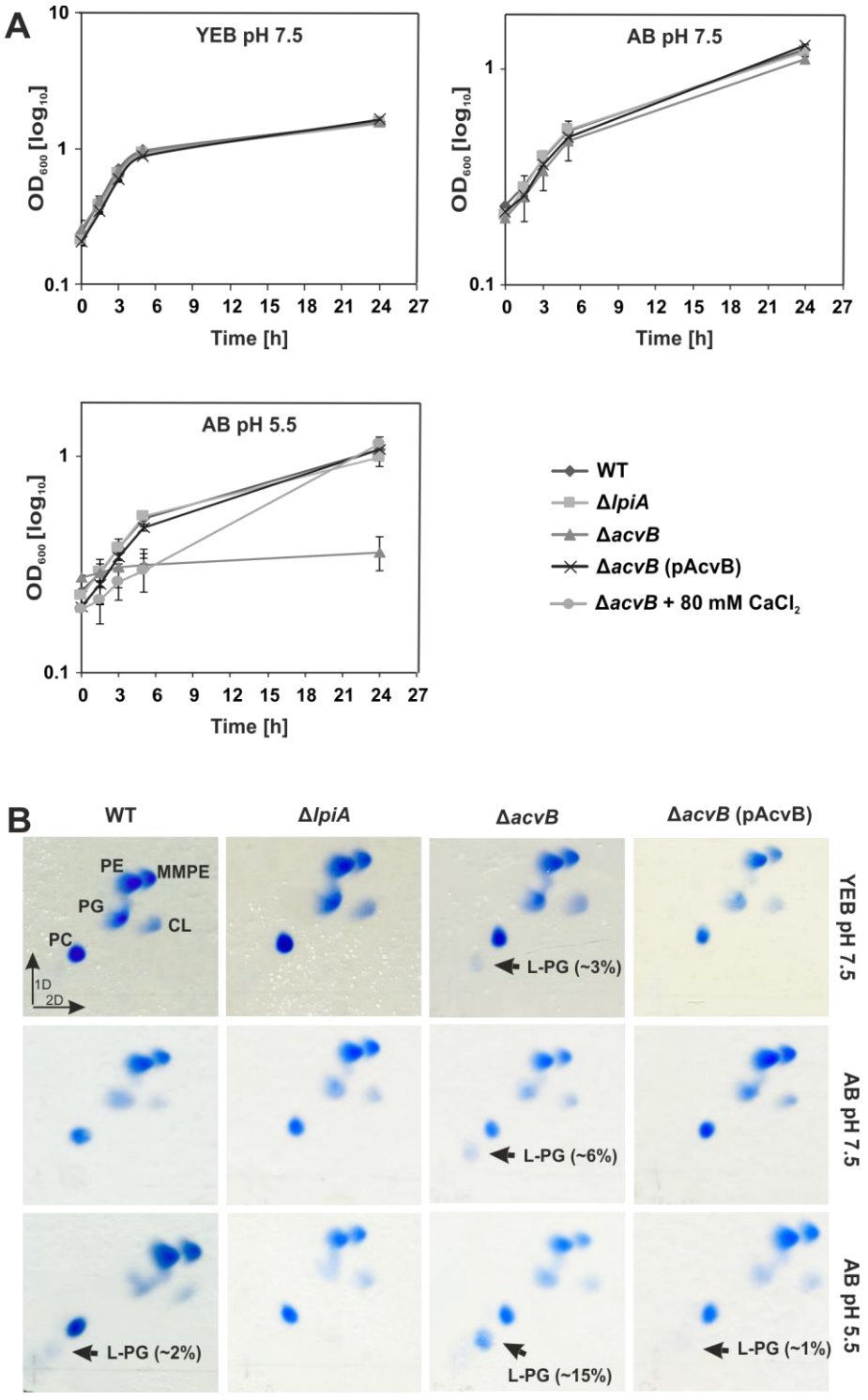

Fig. 6: Growth characteristics, lipid profiles and response to acidic conditions of strains Δ*lpiA* and Δ*acvB*. (A) Growth behaviour of wild type and mutated *A. tumefaciens* strains were analysed in YEB complex medium and in AB minimal medium under neutral and acidic conditions (pH 7.5 and 5.5). The complemented *acvB*-mutant strain carrying pTrC-*acvB* (Δ*acvB* (pAcvB)) was grown in the presence of 0.4 mM IPTG to induce protein expression. Strain Δ*acvB* was grown in the absence or presence of 80 mM $CaCl_2$, which partially restored the impaired growth

of this mutant. Mean value for the growth curves were calculated from results of three independent experiments and error bars show standard errors of the means. (B) After 24 h cultivation, total lipids were extracted from 2 ml of cultures with an adjusted OD_{600} of 3.0 and separated via two-dimensional thin layer chromatography. Phospholipids were visualized with molybdenum blue spray reagent. Mixtures of chloroform:methanol:water (65:25:4) and chloroform:methanol:acetic acid:water (90:15:10:3.5) were used as running solvents for first and second dimension, respectively. L-PG spot intensity was quantified using AlphaEase FC software and normalized relative to the total lipid content. PE, phosphatidylethanolamine; MMPE, monomethyl-PE; PG, phosphatidylglycerol; PC, phosphatidylcholine; CL, cardiolipin; L-PG, lysyl-PG. The TLCs shown are representative examples from at least three independent experiments.

The acvB mutant is unable to induce tumors

The *A. tumefaciens* potato disc assay was used to investigate crown gall tumor formation of strains Δ*lpiA* and Δ*acvB.* Strain Δ*lpiA* produced ~80 tumors per disc like the wild type (Fig. 7A) showing that the presence of L-PG in the bacterial membrane is not a prerequisite of T4SS-mediated transfer of oncogenic T-DNA.

Strain Δ*acvB* was incapable of tumor formation, in full agreement with earlier investigations (Kalogeraki & Winans, 1995, Pan *et al.*, 1995, Wirawan *et al.*, 1993). Loss of virulence in Δ*acvB* was fully restored by complementation with a plasmid encoded *acvB* (compare WT carrying an empty pTrC vector with strain Δ*acvB* (pAcvB)). These data strongly suggest a correlation between lipid homeostasis and the virulence phenotype of Δ*acvB*. Since *A. tumefaciens* transfers T-DNA or virulence proteins by the T4SS, we first analysed the integrity of the T4SS machinery in the mutant strains Δ*acvB* and Δ*lpiA.* Then, the localization of the T4SS complex within the membrane was characterized and finally the influence of individual AcvB amino acid substitutions or deletions was studied on the basis of T-DNA transfer assays.

Key components of the T4SS are present in the acvB mutant Presence of T4SS in the *acvB* mutant was examined using antibodies against the core complex (anti-VirB8 and anti-VirB9) and against the minor component of the T-pilus (anti-VirB5). All targeted proteins were clearly detectable from virulence induced Δ*acvB* cultures, demonstrating that the main components of the T4SS are also produced in the avirulent strain. Crude cellular extracts revealed wild type-like levels of VirB9 and only slightly reduced amounts for VirB8 (Fig. 7B). Furthermore, it was demonstrated that VirB9 and VirB5 exclusively localize in the membrane fraction (Fig. 7C), showing that the overall complex is properly translocated into the bacterial membrane. However,

302 the amount of VirB5 was clearly lowered which might indicate reduced VirB5 synthesis or
303 alternatively an imperfect formation of the fragile T-pilus structure."

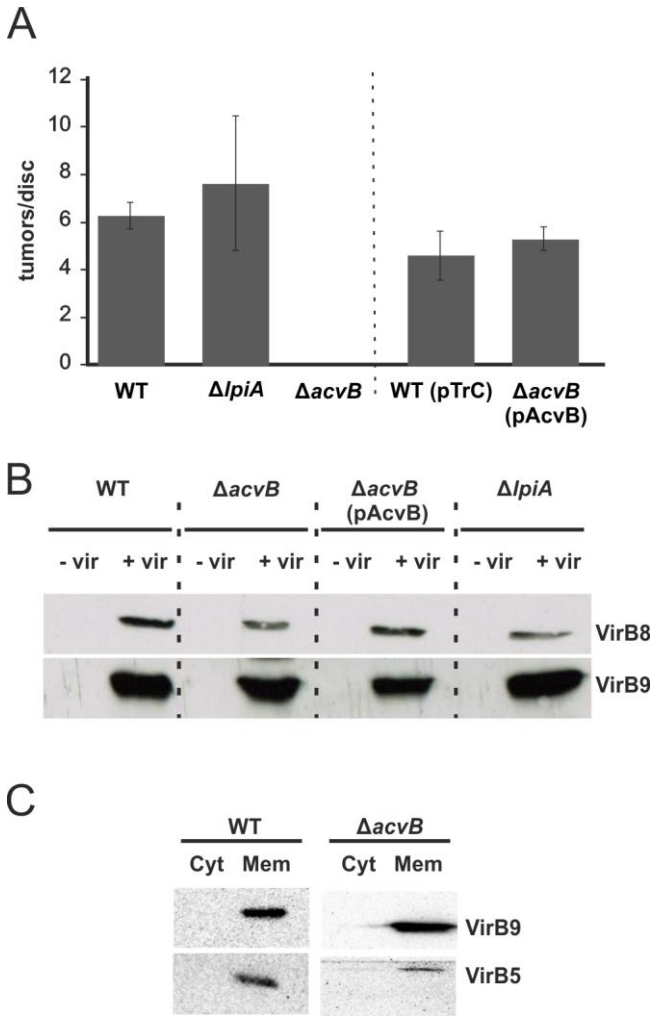

Fig. 7: Tumor-formation defect of the *A. tumefaciens acvB* mutant on potato discs and detection of selected T4SS components. (A) Quantitative tumor-formation assay on potato tuber discs was performed with 10^8 cells/disc. *A. tumefaciens* wild type (WT), Δ*acvB*-mutant, the complemented mutant (Δ*acvB* (pAcvB), and Δ*lpiA* mutant were examined for their tumor formation efficiency on potato discs. Tumorigenesis efficiency is scored by the number of tumors per disc (mean value calculated from results of 55 potato tuber discs for each strain in each independent experiment; error bars show standard errors of the means). (B) Cell extracts and fractionated total membranes (C) of *A. tumefaciens* strains were analysed by Western blotting using VirB protein specific antibodies. Equal loading was ensured by loading the same number of cells per lane (according to optical density) and checking by SDS-PAGE and Coomassie blue stain. – vir, without virulence induction by acetosyringone; + vir, virulence induction by acetosyringone; Cyt, cytosol; Mem, membrane.

304

Increased cellular L-PG levels impair T-DNA transfer

To investigate whether the virulence defect in the *acvB* mutant is related to the L-PG hydrolase activity of AcvB or to a proposed chaperone function, we performed the *Agrobacterium*-mediated transient expression assay AGROBEST with *Arabidopsis* seedlings (Wu *et al.*, 2014) and Δ*acvB* mutant strains, complemented with different *acvB* variants. The β-glucuronidase (GUS) (Narasimhulu *et al.*, 1996, Wu *et al.*, 2014) was used as a reporter to monitor T-DNA-transfer. For that purpose, all investigated *A. tumefaciens* strains contained the T-DNA vector pBISN1 harboring the *gusA*-intron as a reporter. The L-PG content of all strains tested in the GUS assay was determined as described above (Fig 8, insets).

As indicated by stained cotyledons, *Arabidopsis* seedlings were successfully transformed by the wild-type strain containing ~1% L-PG (Fig. 8A). In contrast, the *acvB* mutant with dramatically increased L-PG content (~12%) was unable to transform *Arabidopsis* seedlings (Fig. 8B) confirming the tumor assay results and previously published data (Pan *et al.*, 1995). Obviously, the presented infection assays under neutral or acidic pH conditions (potato disc tumor assay versus GUS assay) revealed an identical virulence phenotype for the *acvB* mutant. Identical results were also observed when T-DNA transfer was analysed in the presence of 80 mM $CaCl_2$ (not shown). L-PG accumulation and loss of transformation capacity was restored by expression of plasmid-encoded wild-type *acvB* or the N-terminally truncated and still catalytically active protein ($AcvB_{232-546}$; with attached natural leader sequence) (Fig. 8C and D and Fig. 5B). Obviously, presence of the C-terminal catalytic domain is sufficient for the T-DNA transfer of *A. tumefacie*ns.

Although the AcvB variant S269A showed significantly reduced activity in our *in vitro* assay (Fig. 5B), the residual activity fully restored the L-PG and virulence phenotype (Fig. 8E).

The *acvB* mutant complemented with the N-terminal domain of AcvB ($AcvB_{1-231}$) produced increased L-PG amounts (~20%) and was unable to transform *Arabidopsis* seedlings similar to the Δ*acvB* mutant (Fig. 8F). Consequently, the N-terminal domain alone is not sufficient to restore T-DNA transfer. L-PG levels of Δ*acvB* strains complemented with the active site point mutated AcvB variants (H33A/N or S336A) (Fig. 5B) were high (5-9%) resulting in strongly reduced transformation capacity (Fig. 8G-I). These experiments revealed a correlation between the L-PG hydrolase activity and the T-DNA transfer capacity of *A. tumefaciens*. A L-PG content of up to ~3% did not seriously interfere with DNA transfer but concentrations above 3% impair

this process. Thus, we hypothesize that the enzymatic activity of AcvB and not a previously postulated chaperone activity is crucial for plant transformation. To further confirm this hypothesis, we overexpressed *lpiA* in the wild-type strain to enhance L-PG production and tested the T-DNA transfer ability of this strain. Similar to the acvB mutant, this strain with a L-PG content of ~7% showed reduced growth and lost its ability to transfer T-DNA (Fig. 8J). From these experiments and the outcome of the overall investigation, we conclude that more than 3% of L-PG in the membrane result in loss of virulence due to impaired T-DNA transfer in *A. tumefaciens.*

Analysis of the overall phospholipid composition for all employed strains showed no drastic alterations with the exception of MMPE (Fig. S2). All strains with increased L-PG amounts revealed an MMPE decrease of about 30% as already indicated in Fig. S1.

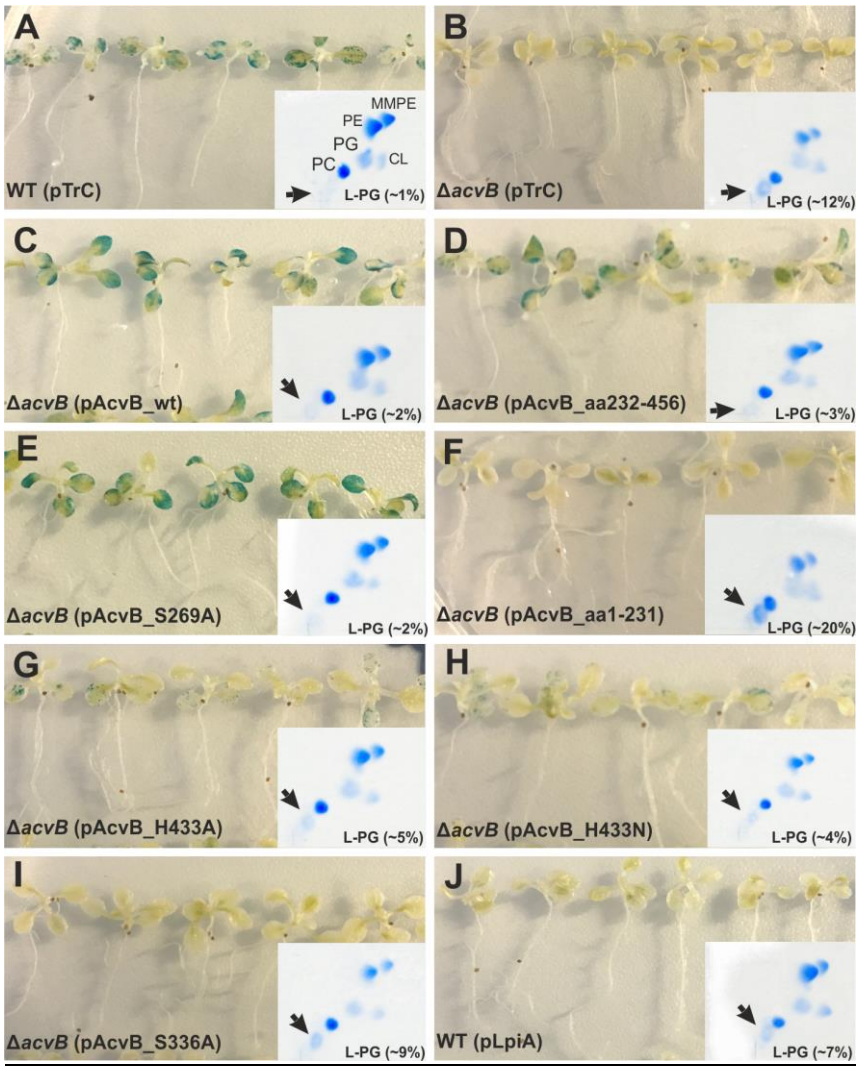

Fig. 8: A*grobacterium*-mediated transient transformation in *Arabidopsis* seedlings. Seven-day-old *Arabidopsis efr-1* seedlings were infected with *Agrobacterium* C58-derivatives carrying pBISN1 and respective pTrC-derivatives for three days before transient GUS expression efficiency was measured by GUS staining. The inset shows the lipid profile of the respective strains with the relative L-PG amount. Lipids from the strains used for infection were isolated, separated and the relative L-PG content was quantified as described in Fig. 6. One representative result for each strain from three independent experiments is shown. (A) WT (pTrC), wild type strain carrying the empty vector pTrC; (B) Δ*acvB* (pTrC), deletion strain carrying the empty vector pTrC, (C) Δ*acvB* (pAcvB_WT), deletion strain complemented with the wild type *acvB* gene; (D) Δ*acvB* (pAcvB_aa232-456), deletion strain complemented with the catalytic C-terminal domain; (E) Δ*acvB* (pAcvB_S269A), deletion strain complemented with the AcvB variant S269A; (F) Δ*acvB* (pAcvB_aa1-231), deletion strain complemented with the N-terminal AcvB part; (G) Δ*acvB* (pAcvB_H433A), deletion strain complemented with the AcvB variant H433A; (H) Δ*acvB* (pAcvB_H433N), deletion strain complemented with the AcvB variant H433N; (I) Δ*acvB* (pAcvB_S336A); deletion strain complemented with the AcvB variant S336A (all plasmid localized *acvB* genes encoding the natural signal sequence) ; (J) WT (pLpiA), wild type strain carrying plasmid encoded L-PG synthase (*lpiA*).

DISCUSSION

Bacterial T4SSs mediate transfer or uptake of DNA, secretion of toxins or injection of virulence factors into host target cells. Accordingly, structural understanding of these sophisticated molecular machines and their inherent controlling by the pathogen (or via the host cell) is of central importance. In this study, we demonstrate that L-PG lipid homeostasis plays a critical role for the *A. tumefaciens* mediated T-DNA transfer.

The physical properties of bacterial membranes must be constantly adapted to changing environmental conditions (Zhang & Rock, 2008). In this context, synthesis of L-PG (e.g. in *S. aureus*, *Bacillus anthracis*, *Bacillus licheniformis*) or of A-PG (e.g. in *P. aeruginosa*) has been described as an important strategy that reduces the overall net negative charge of the membrane, thereby making bacteria less susceptible to cationic antimicrobial peptides, defensins, antimicrobials or acidic conditions (Klein *et al.*, 2009, Maloney *et al.*, 2009, Peschel *et al.*, 2001, Thedieck *et al.*, 2006). For bacterial resistance, the cellular aminoacyl-PG content requires precise tuning. Regulatory circuits for the specific synthesis and hydrolysis of aminoacyl-PGs (A-PG or L-PG/arginyl-PG) have been described in *P. aeruginosa* or *E. faecium* (Arendt *et al.*, 2013, Smith *et al.*, 2013).

In vivo experiments of the present study clearly show that LpiA is responsible for the specific synthesis of L-PG in *A. tumefaciens*. L-PG synthases are transmembrane proteins with a C-terminal cytoplasmic domain responsible for L-PG synthesis (Hebecker *et al.*, 2015). The N-terminal domain, which is anchoring the overall enzyme in the membrane, provides flippase activity (Ernst & Peschel, 2011) (Fig. 9) translocating L-PG from the inner leaflet to the outer leaflet of the membrane. Obviously, the presence of L-PG is not essential for *A. tumefaciens* virulence since the *lpiA* mutant, which is devoid of L-PG, was still able to form tumors on potato discs (Fig. 7A). Cellular L-PG homeostasis in *A. tumefaciens* requires the periplasmic L-PG hydrolase AcvB (Fig. 9). Deletion of *acvB* results in a drastic increase of L-PG accompanied by loss of T-DNA transfer and tumor formation (Fig. 9).

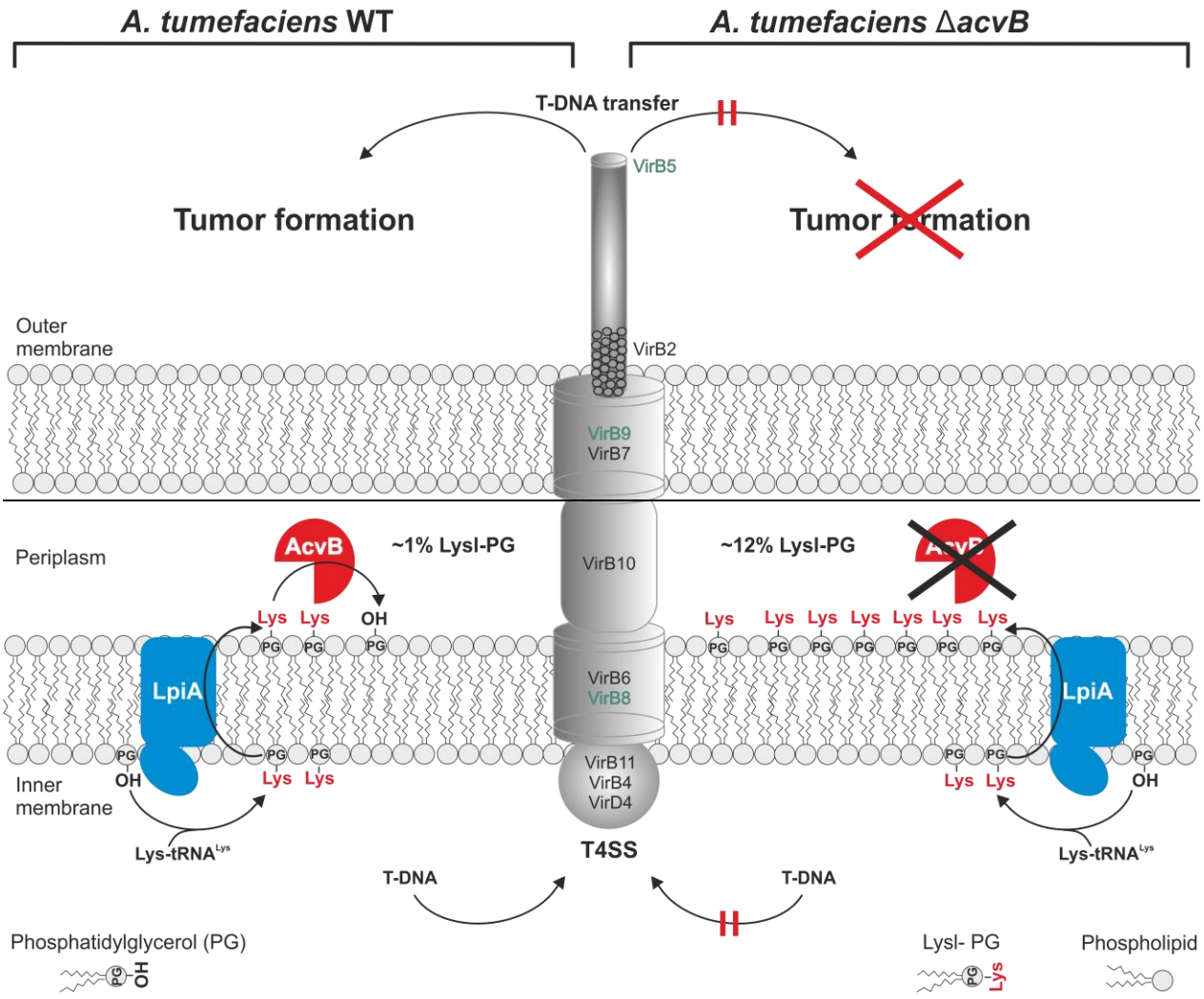

Fig. 9: L-PG-dependent lipid homeostasis affects the T4SS-dependent transfer of T-DNA in *A. tumefaciens*. Schematic representation of the L-PG metabolism at the cytoplasmic membrane. LpiA catalyzes the synthesis of L-PG from PG and Lys-tRNA^{Lys}. L-PG synthases are transmembrane proteins with a C-terminal cytoplasmic domain responsible for L-PG synthesis (Hebecker *et al.*, 2015). The N-terminal domain is anchoring the overall enzyme in the membrane and also provides flippase activity (Ernst & Peschel, 2011). The periplasmic lipid hydrolase AcvB converts L-PG to PG and lysine. AcvB-dependent L-PG homeostasis is relevant for the virulence of *A. tumefaciens*. The related T4SS is schematically depicted and epitopes used for detection of the complex are highlighted in green.

A series of complemented *A. tumefaciens* Δ*acvB* strains allowed for the investigation of virulence phenotypes in response to gradually increasing L-PG levels. Solely strains with an L-PG content of 0 - 3% revealed a fully virulent phenotype (Fig. 7A, Fig. 8 and Fig. 10). An L-PG content of 4 - 5% was accompanied by a strongly reduced virulence phenotype and all strains with more than 5% L-PG were completely avirulent. This was confirmed when the L-PG synthase was

overproduced in the wild type strain (Fig. 8 and Fig. 10). These results might also indicate that the absence of AcvB-dependent L-lysine formation in the periplasm is not responsible for the observed virulence phenotype of the Δ*acvB* strain.

From the present investigation we conclude that AcvB-dependent lipid homeostasis is essential for the T4SS-mediated T-DNA transfer in *A. tumefaciens*.

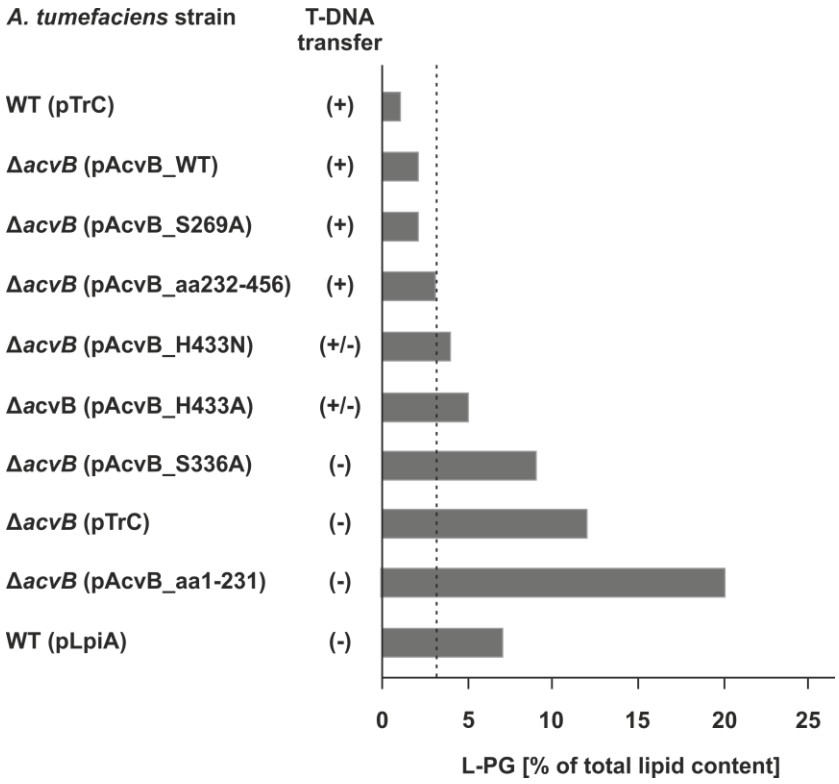

Fig. 10: L-PG content and T-DNA transfer capacity of *A. tumefaciens* strains. The dashed line indicates the L-PG threshold concentration (~3%) above which T-DNA transfer is impaired. Data from GUS assays shown in Fig. 8 are summarized. (+), T-DNA transfer; (+/-), strongly reduced T-DNA transfer; (-), no detectable T-DNA transfer.

But how does the lipid composition of the bacterial cell influence T4SS-mediated T-DNA transfer? It has been shown previously, that sufficient quantities of the phospholipid PC in the membrane of *A. tumefaciens* are a prerequisite for plant infection. A PC-deficient strain showed a virulence defect due to a complete lack of the type IV secretion machinery (Wessel *et al.*, 2006) possibly due to an inactive sensor kinase VirA (Aktas *et al.*, 2014).

The plant symbiosis of *Bradyrhizobium japonicum* or of *Sinorhizobium meliloti* was also shown to be PC-dependent. Depletion of PC in *B. japonicum* drastically reduced the occupancy of

nitrogen-fixing nodules (Minder *et al.*, 2001) and a transcriptional response concerning the RND-type transport system was demonstrated (Hacker *et al.*, 2008). In mutants of *S. meliloti*, which are devoid of PC synthesis formation of nodules was completely prevented (Sohlenkamp *et al.*, 2004). Furthermore, the human pathogen *Brucella abortus* requires PC for virulence (Comerci *et al.*, 2006, Conde-Alvarez *et al.*, 2006). All these lipid-dependent phenotypes might be effectuated by impaired translocation processes at the bacterial membrane. However, the molecular basis for these lipid-dependent symbiosis or virulence phenotypes is still elusive.

On the other hand, lack of membrane-lipids such as ornithine lipids, can accelerate tumor formation in *A. tumefaciens* (Vences-Guzman *et al.*, 2013), or are dispensable for virulence like the anionic lipid cardiolipin (Czolkoss *et al.*, 2016).

With respect to the L-PG-dependent infection phenotypes of the present study, cellular lipid interplay could be influenced at various levels: (I) The transfer rate of the T4SS might be directly affected by the lipid composition of *A. tumefaciens*. The overall net negative charge of the bacterial membrane might be partially compensated in the presence of high cationic L-PG concentrations. Thereby, the activity of the T-DNA transfer machinery would be modulated. (II) The maturation of the functional T4SS might be hampered in the presence of increasing L-PG concentrations. Upon assembly of the secretion machinery, the topology of individual components in the membrane might be influenced by the lipid composition of the cell. Such mechanism has been elucidated for the polytopic membrane protein lactose permease. In cells lacking phosphatidylethanolamine, the N-terminal half of the membrane protein adopted an inverted topology, which only retained to the native membrane topology upon post-assembly synthesis of phosphatidylethanolamine (Bogdanov *et al.*, 2002, Xie *et al.*, 2006, Findlay & Booth, 2017). One further example is the photosynthetic apparatus of *Synechocystis sp.* PCC6803. Functional assembly of this transmembrane complex is not possible if cells lack the phospholipid PG (Hagio *et al.*, 2000, Sato *et al.*, 2000). Furthermore, it was demonstrated recently that the needle-like structure of the bacterial sex F pilus (a conjugative T4SS) is composed as a protein-phospholipid complex (Costa *et al.*, 2016). (III) Individual phospholipids might function as ´signaling molecules´, as also described for eukaryotic systems. With respect to this, the lipolytic activity of AcvB should be also assessed as part of a more globular lipidomic response, which might be also influenced by the host cell.

A broad set of experimental strategies will be required for the molecular understanding of the lipid-dependent virulence of *A. tumefaciens*. At any rate, it seems plausible that lipid homeostasis

plays an important role also for other host microbe interactions. In this context, bacterial lipid metabolism might become also a promising target for the development of new drugs that interfere with the establishment of pathogenic interactions.

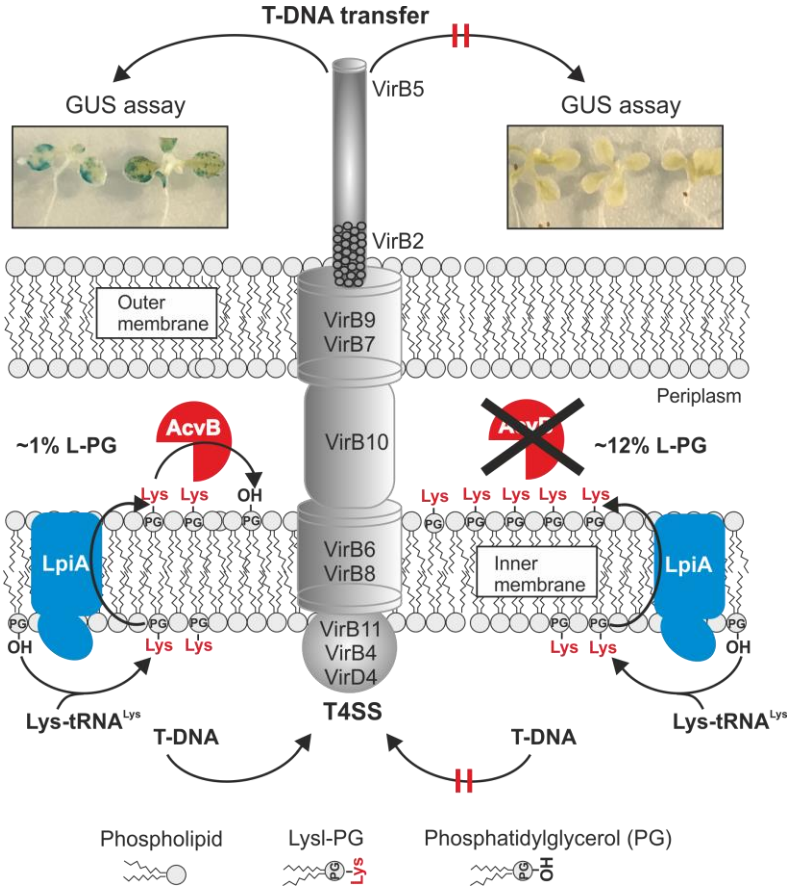

Fig. Graphical abstract

Abbreviated summary: In this study, we show that the virulence factor AcvB is a lysyl-phosphatidylglycerol (L-PG) hydrolase that controls proper L-PG levels in *A. tumefaciens* membranes. Loss of AcvB results in increased L-PG accumulation, which is accompanied with loss of virulence due to abolished T-DNA transfer into plant cells**.**

EXPERIMENTAL PROCEDURES

Analysis of orthologous gene clusters, sequence alignment

The genomic context of *acvB* was analysed using the microbial genome database for the comparative analysis of orthologous groups of genes (MBGD) (Uchiyama *et al.*, 2010). Sequence alignments and identity values were calculated by using ClustalOmega (Sievers *et al.*, 2011).

Media, bacterial strains and cultivation for growth and lipid analysis

E. coli strains (compare Table S2) were grown at 37°C in LB medium (Sambrook & Russell, 2001) supplemented with ampicillin (100 µg ml^{-1}), streptomycin (100 µg ml^{-1}) or spectinomycin (300 µg ml^{-1}) if appropriate. Growth behavior of different *A. tumefaciens* strains was determined in YEB-complex medium and in AB-minimal medium (pH 7.5 and 5.5). Pre-cultures were grown at 30°C over-night in YEB-liquid medium supplemented with 300 µg ml^{-1} spectinomycin if appropriate. Pre-cultures were transferred to fresh YEB and AB-medium (pH 7.5 and 5.5) to prepare main cultures with a starting OD_{600} of 0.2 (media were supplemented with the respective antibiotic and 0.4 mM isopropyl-β-D-thiogalactopyranoside (IPTG, if appropriate). Bacterial growth was monitored for 24 h at 30°C by measuring OD_{600} at different time points (1.5 h, 3 h, 5 h and 24 h). After 24 h growth, 2 ml samples of cultures with an OD_{600} adjusted to 3.0 were collected for lipid analysis.

Subcellular localization of AcvB

To investigate the localization of AcvB in *A. tumefaciens*, a translational fusion of the theoretical N-terminal signal sequence of AcvB and PhoA was constructed. Translated PhoA only shows enzyme activity after translocation to the periplasm. A synthetic gene (Geneart) containing bases 1 – 72 of *acvB* followed by bases 100 – 1,416 from *phoA* (compare Table S1) was synthesized and cloned into the NcoI/HindIII sites of pTRC200 using the In-Fusion HD Cloning technique (Clontech) to yield vector pTRC200_*acvB-phoA*. For control experiments, plasmids pTRC200_native-*phoA* and pTRC200_Δss-*phoA* were generated using oligonucleotide pairs 12/13 and 12/14. These plasmids were used to investigate periplasmic alkaline phosphatase activity by hydrolysis of 5-Brom-4-chlor-3-indolylphosphat (BCIP) in the *A. tumefaciens* C58 wild type background. The resulting 5-bromo-4-chloro-3-indoxyl is further oxidized to the blue

dye 5,5′-dibromo-4,4′-dichloro-indigo (Brickman & Beckwith, 1975). YEB-plates were supplemented with 90 µg ml^{-1} BCIP and 25 mM di-sodium hydrogen phosphate to inhibit the endogenic alkaline phosphatase of *A. tumefaciens* (Bina *et al.*, 1997). Plates were inoculated with an overnight culture of the corresponding *A. tumefaciens* strain and cultivated for 4 days at 30°C. Resulting alkaline phosphatase activity was analysed from whole cells or alternatively after subcellular fractionation. Therefore, 500 ml of the respective cell culture was grown in YEB medium supplemented with 300 µg ml^{-1} spectinomycin and 100 µg ml^{-1} streptomycin to an OD_{578} of 0.5 and induced with 15 µM of IPTG. After 3 h at 30°C, cells were harvested and subcellular fractionation was performed according to (Kang *et al.*, 1994). In all cases, the alkaline phosphatase activity (endogenous periplasmic activity) and malate dehydrogenase activity (endogenous cytosolic activity) of the respective *A. tumefaciens* fractions was determined to evaluate potential cross contamination as detailed in (de Maagd & Lugtenberg, 1986).

Production and purification of recombinant AcvB from the periplasmic fraction of E. coli

Efficient periplasmic overproduction of AcvB in *E. coli* was achieved by exchange of the natural N-terminal leader sequence against the *E. coli* specific PelB sequence. A C-terminal Strep-tag II fusion allowed for purification and detection of the protein. Therefore, base pairs 73 – 1368 of *acvB* (*acvB* gene devoid of its natural leader sequence) were PCR-amplified using oligonucleotides 1/2 and cloned into the NcoI/HindIII site of vector pET22b(+)Strep (Nicke *et al.*, 2013) using the In-Fusion HD Cloning technique (Clontech) to yield vector pET22b(+)Strep_pelB_acvBΔaa1-24. For the production of the C-terminal AcvB domain ($AcvB_{232-456}$), vector pET22b(+)Strep_pelB_acvBΔaa1-230 was constructed analogously (primers 2/3). Variants of the pET22b(+)Strep_pelB_acvBΔaa1-24 plasmid (Table S2) were constructed by site-directed mutagenesis using the the QuickChange kit (Agilent) according to the manufacturer´s instructions (primers 4-11). *E. coli* BL21 (λDE3) (Stratagene) containing pET22b(+)Strep_pelB_acvB (or plasmid variants) was cultivated in 500 ml of LB (100 µg ml^{-1} ampicillin) to an OD_{578} of 0.5. Protein production was induced with 25 µM IPTG for 24 h at 17°C. Cells were harvested, suspended in 50 mM HEPES-NaOH, pH 8.0, 150 mM NaCl, 20% (w/v) D-(+)-sucrose and pellets were stored at -20°C. Thawed cells were suspended in 50 mM HEPES-NaOH, pH 8.0, 150 mM NaCl, 20% (w/v) D-(+)-sucrose containing 2 mg ml^{-1} polymyxin B (Sigma-Aldrich). After 1.5-h incubation at 4°C, the periplasmic fraction was obtained by centrifugation (1.5 h, 20,000 x g, 4°C). Biotinylated host proteins were masked in the

supernatant by 0.4 µM avidin addition (Calbiochem®, Merck). The soluble periplasmic fraction was loaded onto 1 ml of Strep-Tactin® Superflow® resin (IBA) previously equilibrated with 50 mM HEPES-NaOH, pH 8.0, 100 mM NaCl (washing buffer). The resin was washed with 2 x 5 ml washing buffer and the target protein was liberated in the presence of 2.5 mM desthiobiotin (IBA). Elution fractions were dialyzed (20 mM HEPES-NaOH, pH 6.8), concentrated to ~ 3 mg ml^{-1} (Vivaspin 4, 10-kDa cut-off, Sartorius) and the Bradford reagent (Sigma-Aldrich) was used for the determination of protein concentrations.

N-terminal amino acid sequence determination

Automated Edman degradation was used to confirm the identity of purified proteins.

Determination of native molecular mass

Analytical gel permeation chromatography using a Superdex 200 HR 10/30 column in combination with an Äkta purifier system (GE Healthcare) was performed as described elsewhere (Moser *et al.*, 1999).

Thermofluor assay

The thermal stability of recombinant AcvB proteins was investigated by thermal denaturation experiments (Thermofluor assay) as described elsewhere (Niesen *et al.*, 2007).

Esterase activity of AcvB

The following chromogenic nitrophenyl ester compounds were analysed as potential artificial substrate of AcvB: Acetyl-p-nitrophenyl ester (4-nitrophenyl acetate, Sigma-Aldrich) and alanyl-p-nitrophenyl ester (H-Ala-ONP, Bachem). Kinetic formation of p-nitrophenolat was analysed spectroscopically at 400 nm as recently described (Arendt *et al.*, 2013).

AcvB in vitro activity assay

To demonstrate the enzymatic activity of AcvB (or of variant AcvB proteins), an *in vitro* activity assay was elucidated. A micellar substrate mixture containing 5.13 mM L-PG was prepared as follows: 1 mg of 18:1 L-PG (1,2-dioleoyl-*sn*-glycero-3-[phospho-*rac*-(3-lysyl(1-glycerol))], Avanti Polar Lipids) was mixed with 200 µl of dialysis buffer containing 3 mg ml^{-1} Triton™ X-

100 (Sigma-Aldrich) for 15 min at 37°C under vigorous shaking. A typical 160 µl assay contained 80 µl of a 20 µM AcvB solution (or variant AcvB protein) in 20 mM of HEPES-NaOH, pH 6.8 and 80 µl of the L-PG substrate mixture. Assays were incubated at 37°C and 1,000 rpm. After 30 min, reactions were stopped by addition of 400 µl methanol and 200 µl chloroform. Phospholipids were extracted by the method of Bligh and Dyer (Bligh & Dyer, 1959), separated by two-dimensional thin layer chromatography and visualized by molybdatophosphoric acid and ninhydrin staining as described in (Klein *et al.*, 2009). Authentic L-PG or PG (16:0-18:1 PG, 1-palmitoyl-2-oleoyl-*sn*-glycero-3-phospho-(1'-*rac*-glycerol), Avanti Polar Lipids) samples were processed accordingly. Notice that L-PG samples always contain minor amounts of PG and L-lysine as a result of spontaneous hydrolysis. Employed L-PG fractions contain up to 15 % of an acyl migration isomer as a result of the employed chemical synthesis strategy of the manufacturer (Avanti Polar Lipids).

Alternatively, L-PG and L-lysine were identified on one-dimensional thin layer chromatography plates after ninhydrin staining: 5 µl-samples of the *in vitro* assay were directly spotted onto the plate at various time points (1, 2, 3, 4, 5, 10, 20, 30 and 60 min) and separated according to (Arendt *et al.*, 2013). In parallel, 5 µl L-lysine samples with concentrations ranging from X to Y (Fluka) were processed and subsequently quantified by densitometry using the Gelscan software package (BioSciTec). In all cases, the Strep-tag-II protein (3.1 kDa) was used as a control. All activity measurements were reproduced in at least three independent experiments.

Construction of A. tumefaciens deletion strains ΔlpiA, ΔacvB, and complementation variants

Markerless *lpiA*- and *acvB*-deletion mutants were generated in *A. tumefaciens* strain C58 via double crossover using the suicide vector pK19mobsacB (Schäfer *et al.*, 1994) as described in (Wessel *et al.*, 2006).The corresponding *lpiA* and *acvB* up- and downstream gene regions (~ 400 bp) were amplified using the oligonucleotide pairs 17-20 and 21-24 (Table S1). PCR-fragments were cloned into pK19mobsacB and the resulting plasmids pBO1915 (*acvB*) and pBO1916 (*lpiA*) were introduces into *A. tumefaciens* by electroporation. Single-crossover integration mutants were selected on LB plates containing kanamycin. Kanaymcin-resistant single colonies were cultivated without antibiotic for 24 h in liquid LB medium and plated on LB plates containing 10% (w/v) sucrose to select for plasmid excision by double-crossover events. Kanamycin-sensitive colonies were checked for the targeted deletion by colony-PCR and Southern blot analysis.

For subsequent complementation of strain Δ*acvB*, primers 25/26 were used to clone vector pTRC200_acvB_Strep on the basis of plasmid pTRC200 (Schmidt-Eisenlohr *et al.*, 1999a). (Table S1 and S2). Site-directed mutagenesis of *acvB* was performed as described above using primer pairs 4/5 to 10/11. Complementation plasmids were transferred into *A. tumefaciens* strain Δ*acvB* via electroporation.

Construction of A. tumefaciens lpiA overexpression strain

The *lpiA* coding region was amplified from chromosomal DNA using the primer pair 27/28 (Table S1). The PCR product (2,601 bp) was cloned via the NcoI and XbaI restriction sites into the IPTG inducible pTrC200 (Schmidt-Eisenlohr *et al.*, 1999b) expression vector resulting in plasmid pBO1919. The pBO1919 was transferred into wild type *A. tumefaciens*.

Cultivation of A. tumefaciens strains for growth and lipid analysis

Growth behavior of different *A. tumefaciens* strains was determined in YEB-complex medium and in AB-minimal medium (pH 7.5 and 5.5). Pre-cultures were grown at 30°C over-night in YEB-liquid medium supplemented with 300 µg ml^{-1} spectinomycin, if appropriate. Pre-cultures were transferred to fresh YEB and AB-medium (pH 7.5 and 5.5) to prepare main cultures with a starting OD_{600} of 0.2 (media were supplemented with the respective antibiotic and 0.4 mM IPTG, if appropriate). Bacterial growth was monitored for 24 h at 30°C by measuring OD_{600} at different time points (1.5 h, 3 h, 5 h and 24 h). After 24 h growth, 2 ml samples of cultures with an OD_{600} adjusted to 3.0 were collected for lipid analysis.

Lipid extraction and two-dimensional thin layer chromatography of A. tumefaciens cells

Phospholipids of *A. tumefaciens* C58 wild type and derivatives grown under different conditions were isolated according to (Bligh & Dyer, 1959). Briefly, 2 ml cultures with an OD_{600} adjusted to 3.0 were harvested by centrifugation and washed with 500 µl of water. Cells were resuspended in 100 µl of water and homogenized with 375 µl of methanol:chloroform (2:1) before 100 µl of water and 100 µl of chloroform were added. Samples were briefly vortexed and centrifuged for 5 minutes at 13,000 rpm. The lower organic phase was collected and dried under vacuum. The lipid pellets were resuspended in 15 µl of methanol:chloroform (1:1) and spotted onto a HPTLC silica gel 60 plate (Merck, Darmstadt, Germany). For two-dimensional dimensional thin layer

chromatography, mixtures of chloroform:methanol:water (65:25:4) and chloroform:methanol:acetic acid:water (90:15:10:3.5) were used as running solvents for first and second dimension, respectively. For the visualization of the phospholipids, plates were stained with molybdenum blue reagent (Sigma-Aldrich). Lysyl-phosphatidylgylcerol (L-PG, C18:1, Avanti Polar Lipids) was used as lipid standard. Relative intensities of L-PG spots were determined using AlphaEase FC software.

Potato disc tumor-induction assay

A. tumefaciens-induced tumorigenesis on potato tuber discs was determined according to (Wu *et al.*, 2008). Briefly, pre-cultures of the respective *A. tumefaciens* strains were grown overnight at 30°C in 5 ml YEB complex medium (strains containing pTrC-derivatives were cultivated with 300 µg ml^{-1} spectinomycin). The overnight cultures were diluted to an OD_{600} of 0.1 in 10 ml YEB medium and cells were cultivated to an OD_{600} of 1.0 (medium contained 300 µg ml^{-1} spectinomycin if appropriate). In case of pTrC-*acvB* containig strains, 0.4 mM IPTG was added at an OD_{600} of 0.4 to induce *acvB* expression. Cells were washed once with 1x PBS buffer and resuspended in concentrations of 10^8 cells/ml in 1x PBS buffer for inoculation. The surface of peeled potatoes (type Marabel, new crop) was disinfected by immersion in 0.625% (w/v) sodium hypochlorite for 5 min and 2 washing steps with sterile water were performed. Cylinders, which were cut out from potato tubers using a sterile cork borer were cut into discs of ~0.4 cm thickness. The discs were placed on water agar and each disc was infected with 10 µl of the bacterial cell suspension containing 10^8 cells/ml. The petri dishes were sealed and incubated in a phytochamber (80 µE light energy, 16 h light/8 h dark period, humidity of 30-45%) at 23°C for 2 days. Discs were transferred to water agar containing 100 µg ml^{-1} ticarcillin to kill the bacteria and incubation was preceded in the phytochamber for 3 weeks before tumors were counted.

Agrobacterium-mediated transient transformation in Arabidopsis seedlings

The T-DNA transfer capability of different *A. tumefaciens* strains into plant cells was analysed by *Arabidopsis* seedlings infection assays according to the AGROBEST method (Wu *et al.*, 2014). The T-DNA vector pBISN1 harboring the *gusA*-intron (Narasimhulu *et al.*, 1996) was transferred by electroporation into different *A. tumefaciens* C58 strains (wt, Δ*lpiA*, Δ*acvB*, complemented Δ*acvB* with ptrC-*acvB* derivatives and WT carrying ptrC-*lpiA*) to infect 7-day-old seedlings, and

β-glucuronidase (GUS) activity was determined to monitor transient expression efficiency at 3 days post-infection (dpi). *Arabidopsis thaliana efr*-1 seeds were sterilized in 50% (v/v) bleach containing 0.05% (v/v) Triton™ X-100 for 10 min and subsequently rinsed 5-times with sterile water. Seeds were incubated at 4°C for 4 days. After cold-treatment, 10 seeds were transferred to each well of a 6-well plate, filled with 1 ml MS medium (2.17 g MS salt (PhytoTechnology Laboratories®, M524), 5 g sucrose, pH 5.7) for germination in a phytochamber (80 µE light energy, 16 h light/8 h dark period) at 23°C for 7 days. Pre-cultures of the respective *A. tumefaciens* strains grown 20 h at 28°C in 523 liquid medium (10 g sucrose, 8 g casein enzymatic hydrolysate (Sigma 22090), 4 g yeast extract, 3 g K_2HPO_4, 0.3 g $MgSO_4$ x $7H_2O$, pH 7.0) with 50 µg ml^{-1} kanamycin (and 300 µg ml^{-1} spectinomycin if appropriate) were pelleted. Cells were resuspended to an OD_{600} of 0.2 in AB-MES pH 5.5 medium (3 g K_2HPO_4,1 g NaH_2PO_4, 1 g NH_4Cl, 0.3 g $MgSO_4$ x $7H_2O$, 0.15 g KCl, 0.01g $CaCl_2$, 2.5 mg $FeSO_4$ x $7H_2O$, 9.76 g MES (2-(*N*-morpholine) ethanesulfonic acid), 20 g glucose) supplemented with 200 µM acetosyringone. Plasmid-encoded AcvB synthesis in the complemented strains was induced with 0.4 mM IPTG. Cultivation was preceded at 28°C for 16 h to induce *vir* gene expression. If required, medium was supplemented with 80 mM $CaCl_2$ (for Δ*acvB*). Cells were sedimented and resuspended to an OD_{600} of 0.02 in infection medium (50 ml MS medium, 50 ml AB-MES medium, 200 µM AS, pH 5.5). If required, infection medium was supplemented with 80 mM CaCl2 (for Δ*acvB*). The MS medium containing the seedlings was replaced by 1 ml of the respective *A. tumefaciens* suspension in infection medium and co-cultivation was performed in a phytochamber (conditions see above) at 23°C for 3 days. The seedlings were incubated with 500 µl GUS staining solution (0.5 mM, $K_3Fe(CN)_6$, 0.5 mM, $K_4Fe(CN)_6$, 0.1% (v/v) Triton™ X- 100, 10 mM EDTA, 1 mM 5-bromo-4-chloro-3-indolyl-β-D-glucuronide, 0.1 M $NaPO_4$ buffer, pH 7.0) at 37°C for 6 h to visualize GUS activity. For lipid analysis of the strains, 2 ml samples with an adjusted OD_{600} of 3.0 were used.

Detection of VirB-proteins in cell extracts

Overnight cultures of *A. tumefaciens* strain C58 (wild type) and derivatives in YEB complex medium were washed twice with AB minimal medium and inoculated to an OD_{600} of 0.1 in AB minimal medium pH 5.5 supplemented with 1% (w/v) glucose. When the cultures reached an OD_{600} of 0.2, virulence was induced by addition of 0.1 mM acetosyringone (Sigma-Aldrich) and cells were further incubated at 23°C for 18 h. Cultures contained 300 µg ml^{-1} spectinomycin and

644 0.4 mM IPTG if appropriate (strains with pTrC-drivatives). For VirB-protein detection, 1 ml of
645 virulence induced and non-induced *A. tumefaciens* cells were harvested and resuspended in
646 sodium dodecyl sulfate (SDS) loading buffer in relation to the final OD_{600}. An OD_{600} value of 1.0
647 thereby equaled 100 µl SDS loading buffer. Samples were heated to 95°C for 10 min before equal
648 amounts of extracts were separated by SDS-PAGE (12.5%-polyacrylamide gel) followed by
649 Western blot analysis and chemiluminescence detection (ECL). VirB8- and VirB9-proteins were
650 detected using *A. tumefaciens* specific antisera (VirB8: 1/100,000; VirB9: 1/10,000) and
651 secondary goat anti-rabbit IgG (H+L)-HRP conjugate (Bio-Rad, Hercules, CA, USA).

652 ***VirB-protein detection in membrane fractions***

653 *A. tumefaciens* wild type and *acvB*-mutant cultures were grown under virulence induced
654 conditions described above and OD_{600} was adjusted to 4.0. Cells were harvested at 4°C, cell
655 pellets were washed and resuspended in 700 µl 50 mM Tris-HCl, pH 7.4. 1 mM PMSF and
656 1.5 mg ml^{-1} lysozyme were added and cells were further incubated for 90 minutes at 4°C. After
657 cell disruption by ultrasonication using a VialTweeter instrument (Hielscher), cell debris was
658 removed by centrifugation at 20,000 g at 4°C for 15 minutes. Membranes were pelleted via
659 ultracentrifugation at 320,000 g for 90 minutes at 4°C. 200 µl of supernatant were transferred to a
660 fresh microcentrifuge tube and stored for further analysis (Cyt). The Membrane pellet was
661 resolved in 600 µl lysis and separation buffer from the CelLytic MEM Protein Extraction Kit
662 (Sigma-Aldrich) containing 6 µl of the provided protease inhibitor cocktail (Mem). For SDS-
663 PAGE and Western blot analysis of the membrane preparation samples, proteins were
664 precipitated with chloroform/methanol. Briefly, samples were mixed with 4x volumes of
665 methanol before 1x volume of chloroform and 3x volumes water were added and mixed. The
666 samples were centrifuged at 20,000 g for 6 minutes at room temperature. The upper layer was
667 removed and 3x volumes of methanol were added to the pellet. After centrifugation at 20,000 g
668 for 6 minutes and evaporation of methanol in a SpeedVac system, protein pellets were resolved in
669 1x SDS sample buffer (1 M Tris, pH 6.5), 50% glycerol (v/v), 10% SDS (w/v), 0.5% bromphenol
670 blue (w/v) and 5% β-mercaptoethanol (v/v)). Equal volumes of fractions were analysed by SDS-
671 PAGE and Western blot analysis. VirB5 and VirB9 were detected using protein-specific
672 antibodies (rabbit) and secondary goat anti-rabbit IgG (H+L)-HRP conjugate (Bio-Rad). Protein
673 signals were visualized using Luminata Forte Western HRP substrate (Merck-Millipore). For
674 signal detection, a ChemiImager Ready system (Alpha Innotec) was used.

AUTHOR CONTRIBUTIONS

J.M., M.A., F.N., D.J. and D.W.H. designed research. M.K.G., S.H., S.C., C.F. and M.W. conducted experiments and analysed the data. J.M., M.A. and F.N. wrote the paper. All authors analysed the results and approved the final version of the manuscript.

References

Aktas, M., L. Danne, P. Möller & F. Narberhaus, (2014) Membrane lipids in *Agrobacterium tumefaciens*: biosynthetic pathways and importance for pathogenesis. *Front Plant Sci* **5**: 109.

Arendt, W., M.K. Groenewold, S. Hebecker, J.S. Dickschat & J. Moser, (2013) Identification and characterization of a periplasmic aminoacyl-phosphatidylglycerol hydrolase responsible for *Pseudomonas aeruginosa* lipid homeostasis. *J Biol Chem.* **288**: 24717-24730.

Arendt, W., S. Hebecker, S. Jäger, M. Nimtz & J. Moser, (2012) Resistance phenotypes mediated by aminoacyl-phosphatidylglycerol synthases. *J Bacteriol* **194**: 1401-1416.

Atmakuri, K., Z. Ding & P.J. Christie, (2003) VirE2, a type IV secretion substrate, interacts with the VirD4 transfer protein at cell poles of *Agrobacterium tumefaciens*. *Mol Microbiol* **49**: 1699-1713.

Bina, J.E., F. Nano & R.E. Hancock, (1997) Utilization of alkaline phosphatase fusions to identify secreted proteins, including potential efflux proteins and virulence factors from *Helicobacter pylori*. *FEMS Microbiol. Lett.* **148** 63-68.

Bligh, E.G. & W.J. Dyer, (1959) A rapid method of total lipid extraction and purification. *Can J Biochem Physiol* **37**: 911-917.

Bogdanov, M., P.N. Heacock & W. Dowhan, (2002) A polytopic membrane protein displays a reversible topology dependent on membrane lipid composition. *EMBO J* **21**: 2107-2116.

Brickman, E. & J. Beckwith, (1975) Analysis of the regulation of *Escherichia coli* alkaline phosphatase synthesis using deletions and phi80 transducing phages. *J. Mol. Biol.* **96**: 307-316.

Cascales, E. & P.J. Christie, (2003) The versatile bacterial type IV secretion systems. *Nat Rev Microbiol.* **1**: 137-149.

Cascales, E. & P.J. Christie, (2004) Definition of a bacterial type IV secretion pathway for a DNA substrate. *Science* **304**: 1170-1173.

Chandran Darbari, V. & G. Waksman, (2015) Structural Biology of Bacterial Type IV Secretion Systems. *Annual review of biochemistry* **84**: 603-629.

Christie, P.J., (2004) Type IV secretion: the *Agrobacterium* VirB/D4 and related conjugation systems. *Biochim Biophys Acta.* **1694**: 219–234.

Christie, P.J. & E. Cascales, (2005) Structural and dynamic properties of bacterial type IV secretion systems (review). *Mol Membr Biol.* **22**: 51-61.

Comerci, D.J., S. Altabe, D. de Mendoza & R.A. Ugalde, (2006) Brucella abortus synthesizes phosphatidylcholine from choline provided by the host. *J Bacteriol* **188**: 1929-1934.

Conde-Alvarez, R., J. Grilló María, P. Salcedo Suzana, J. De Miguel María, E. Fugier, P. Gorvel Jean, I. Moriyón & M. Iriarte, (2006) Synthesis of phosphatidylcholine, a typical eukaryotic phospholipid, is necessary for full virulence of the intracellular bacterial parasite Brucella abortus. *Cell Microbiol* **8**: 1322-1335.

Costa, T.R.D., A. Ilangovan, M. Ukleja, A. Redzej, J.M. Santini, T.K. Smith, E.H. Egelman & G. Waksman, (2016) Structure of the Bacterial Sex F Pilus Reveals an Assembly of a Stoichiometric Protein-Phospholipid Complex. *Cell* **166**: 1436-1444.e1410.

Czolkoss, S., C. Fritz, G. Hölzl & M. Aktas, (2016) Two Distinct Cardiolipin Synthases Operate in *Agrobacterium tumefaciens. PLoS ONE* **11**: e0160373. doi:0160310.0161371/journal.pone.0160373.

de Maagd, R.A. & B. Lugtenberg, (1986) Fractionation of Rhizobium leguminosarum cells into outer membrane, cytoplasmic membrane, periplasmic, and cytoplasmic components. *J Bacteriol* **167**: 1083-1085.

Ernst, C.M. & A. Peschel, (2011) Broad-spectrum antimicrobial peptide resistance by MprF-mediated aminoacylation and flipping of phospholipids. *Mol Microbiol* **80**: 290-299.

Fields, R.N. & H. Roy, (2017) Deciphering the tRNA-dependent lipid aminoacylation systems in bacteria: Novel components and structural advances. *RNA Biol*: 1-12.

Findlay, H.E. & P.J. Booth, (2017) The folding, stability and function of lactose permease differ in their dependence on bilayer lipid composition. *Scientific Reports* **7**: 13056.

Gede Putu Wirawan, I. & M. Kojima, (1996) A Chromosomal Virulence Gene (acvB) Product of *Agrobacterium tumefaciens* That Binds to a T-Strand to Mediate Its Transfer to Host Plant Cells. *Biosci Biotechnol Biochem* **60**: 44-49.

Grohmann, E., P.J. Christie, G. Waksman & S. Backert, (2018) Type IV secretion in Gram-negative and Gram-positive bacteria. *Mol Microbiol* **107**: 455-471.

Ha, B.-Y., (2001) Stabilization and destabilization of cell membranes by multivalent ions. *Physical Review E* **64**: 051902.

Hacker, S., J. Godeke, A. Lindemann, S. Mesa, G. Pessi & F. Narberhaus, (2008) Global consequences of phosphatidylcholine reduction in Bradyrhizobium japonicum. *Mol Genet Genomics* **280**: 59-72.

Hagio, M., Z. Gombos, Z. Varkonyi, K. Masamoto, N. Sato, M. Tsuzuki & H. Wada, (2000) Direct evidence for requirement of phosphatidylglycerol in photosystem II of photosynthesis. *Plant Physiol* **124**: 795-804.

Hebecker, S., W. Arendt, I.U. Heinemann, J.H. Tiefenau, M. Nimtz, M. Rohde, D. Soll & J. Moser, (2011) Alanyl-phosphatidylglycerol synthase: mechanism of substrate recognition during tRNA-dependent lipid modification in Pseudomonas aeruginosa. *Mol Microbiol* **80**: 935-950.

Hebecker, S., J. Krausze, T. Hasenkampf, J. Schneider, M. Groenewold, J. Reichelt, D. Jahn, D.W. Heinz & J. Moser, (2015) Structures of two bacterial resistance factors mediating tRNA-dependent aminoacylation of phosphatidylglycerol with lysine or alanine. *Proc Natl Acad Sci U S A.* **112**: 10691-10696.

Heckel, B.C., A.D. Tomlinson, E.R. Morton, J.H. Choi & C. Fuqua, (2014) *Agrobacterium tumefaciens* exoR controls acid response genes and impacts exopolysaccharide synthesis, horizontal gene transfer, and virulence gene expression. *J Bacteriol* **196**: 3221-3233.

Hoffman, C.S. & A. Wright, (1985) Fusions of secreted proteins to alkaline phosphatase: an approach for studying protein secretion. *Proc Natl Acad Sci U S A* **82**: 5107-5111.

Hooykaas, P.J.J. & A.G.M. Beijersbergen, (1994) The Virulence System of *Agrobacterium tumefaciens*. *Annu Rev Phytopathol* **32**: 157-181.

Kalogeraki, V.S. & S.C. Winans, (1995) The octopine-type Ti plasmid pTiA6 of *Agrobacterium tumefaciens* contains a gene homologous to the chromosomal virulence gene *acvB*. *J. Bacteriology* **177**: 892–897.

Kang, H.W., I.G. Wirawan & M. Kojima, (1994) Cellular localization and functional analysis of the protein encoded by the chromosomal virulence gene(acvB) of *Agrobacterium tumefaciens*. *Biosci Biotechnol Biochem* **58**: 2024-2032.

Klein, S., C. Lorenzo, S. Hoffmann, J.M. Walther, S. Storbeck, T. Piekarski, B.J. Tindall, V. Wray, M. Nimtz & J. Moser, (2009) Adaptation of Pseudomonas aeruginosa to various conditions includes tRNA-dependent formation of alanyl-phosphatidylglycerol. *Mol Microbiol* **71**: 551-565.

774 Maloney, E., D. Stankowska, J. Zhang, M. Fol, Q.J. Cheng, S. Lun, W.R. Bishai, M.
775 Rajagopalan, D. Chatterjee & M.V. Madiraju, (2009) The two-domain LysX protein of
776 *Mycobacterium tuberculosis* is required for production of lysinylated
777 phosphatidylglycerol and resistance to cationic antimicrobial peptides. *PLoS Pathog* **5**:
778 e1000534.
779 Minder, A.C., K.E. de Rudder, F. Narberhaus, H.M. Fischer, H. Hennecke & O. Geiger, (2001)
780 Phosphatidylcholine levels in Bradyrhizobium japonicum membranes are critical for an
781 efficient symbiosis with the soybean host plant. *Mol Microbiol* **39**: 1186-1198.
782 Morris, R.O., (1986) Genes specifying auxin and cytokinin biosynthesis in phytopathogens.
783 *Annu. Rev. Plant Physiol.* **37**: 509-538.
784 Moser, J., S. Lorenz, C. Hubschwerlen, A. Rompf & D. Jahn, (1999) Methanopyrus kandleri
785 glutamyl-tRNA reductase. *J Biol Chem* **274**: 30679-30685.
786 Narasimhulu, S.B., X.B. Deng, R. Sarria & S.B. Gelvin, (1996) Early transcription of
787 *Agrobacterium* T-DNA genes in tobacco and maize. *Plant Cell* **8**: 873-886.
788 Nicke, T., T. Schnitzer, K. Münch, J. Adamczack, K. Haufschildt, S. Buchmeier, M. Kucklick, U.
789 Felgenträger, L. Jänsch, K. Riedel & G. Layer, (2013) Maturation of the cytochrome cd1
790 nitrite reductase NirS from *Pseudomonas aeruginosa* requires transient interactions
791 between the three proteins NirS, NirN and NirF. *Biosci Rep.* **33**: e00048. doi:
792 00010.01042/BSR20130043.
793 Nielsen, H., (2017) Predicting Secretory Proteins with SignalP. *Methods Mol Biol* **1611**: 59-73.
794 Niesen, F.H., H. Berglund & M. Vedadi, (2007) The use of differential scanning fluorimetry to
795 detect ligand interactions that promote protein stability. *Nature Protocols* **2**: 2212–2221.
796 Pan, S.Q., S. Jin, M.I. Boulton, M. Hawes, M.P. Gordon & E.W. Nester, (1995) An
797 *Agrobacterium* virulence factor encoded by a Ti plasmid gene or a chromosomal gene is
798 required for T-DNA transfer into plants. *Mol Microbiol.* **17**: 259-269.
799 Pantoja, M., L. Chen, Y. Chen & E.W. Nester, (2002) *Agrobacterium* type IV secretion is a two-
800 step process in which export substrates associate with the virulence protein VirJ in the
801 periplasm. *Mol Microbiol.* **45**: 1325–1335.
802 Peschel, A., R.W. Jack, M. Otto, L.V. Collins, P. Staubitz, G. Nicholson, H. Kalbacher, W.F.
803 Nieuwenhuizen, G. Jung, A. Tarkowski, K.P. van Kessel & J.A. van Strijp, (2001)
804 *Staphylococcus aureus* resistance to human defensins and evasion of neutrophil killing
805 via the novel virulence factor MprF is based on modification of membrane lipids with l-
806 lysine. *J Exp Med* **193**: 1067-1076.
807 Reeve, W.G., L. Brau, J. Castelli, G. Garau, C. Sohlenkamp, O. Geiger, M.J. Dilworth, A.R.
808 Glenn, J.G. Howieson & R.P. Tiwari, (2006) The *Sinorhizobium medicae* WSM419 *lpiA*
809 gene is transcriptionally activated by FsrR and required to enhance survival in lethal acid
810 conditions. *Microbiology* **152**: 3049-3059.
811 Roy, H., (2009) Tuning the properties of the bacterial membrane with aminoacylated
812 phosphatidylglycerol. *IUBMB Life* **61**: 940-953.
813 Roy, H. & M. Ibba, (2009) Broad range amino acid specificity of RNA-dependent lipid
814 remodeling by multiple peptide resistance factors. *J Biol Chem* **284**: 29677-29683.
815 Sambrook, J. & D.W. Russell, (2001) *Molecular cloning: a laboratory manual*. Cold Spring
816 Harbor Laboratory Press, Cold Spring Harbor.
817 Sato, N., M. Hagio, H. Wada & M. Tsuzuki, (2000) Requirement of phosphatidylglycerol for
818 photosynthetic function in thylakoid membranes. . *Proc Natl Acad Sci U S A* **97**: 10655-
819 10660.
820 Schäfer, A., A. Tauch, W. Jäger, J. Kalinowski, G. Thierbach & A. Pühler, (1994) Small
821 mobilizable multi-purpose cloning vectors derived from the *Escherichia coli* plasmids

pK18 and pK19: selection of defined deletions in the chromosome of *Corynebacterium glutamicum*. *Gene* **145**: 69–73.

Schmidt-Eisenlohr, H., N. Domke, C. Angerer, G. Wanner, P.C. Zambryski & C. Baron, (1999a) Vir proteins stabilize VirB5 and mediate its association with the T pilus of *Agrobacterium tumefaciens*. . *J. Bacteriol.* **181**: 7485–7492.

Schmidt-Eisenlohr, H., N. Domke & C. Baron, (1999b) TraC of IncN plasmid pKM101 associates with membranes and extracellular high-molecular-weight structures in Escherichia coli. *J Bacteriol* **181**: 5563-5571.

Sievers, F., A. Wilm, D.G. Dineen, T.J. Gibson, K. Karplus, W. Li, R. Lopez, H. McWilliam, M. Remmert, J. Söding, J.D. Thompson & D. Higgins, (2011) Fast, scalable generation of high-quality protein multiple sequence alignments using Clustal Omega *Molecular Systems Biology* **7**: 539.

Sigrist, C.J., E. de Castro, L. Cerutti, B.A. Cuche, N. Hulo, A. Bridge, L. Bougueleret & I. Xenarios, (2013) New and continuing developments at PROSITE. *Nucleic Acids Res* **41**: D344-347.

Smith, A.M., J.S. Harrison, K.M. Sprague & H. Roy, (2013) A conserved hydrolase responsible for the cleavage of aminoacylphosphatidylglycerol in the membrane of Enterococcus faecium. *J Biol Chem* **288**: 22768-22776.

Sohlenkamp, C., K.E.E. de Rudder & O. Geiger, (2004) Phosphatidylethanolamine Is Not Essential for Growth of Sinorhizobium meliloti on Complex Culture Media. *J Bacteriol* **186**: 1667-1677.

Thedieck, K., T. Hain, W. Mohamed, B.J. Tindall, M. Nimtz, T. Chakraborty, J. Wehland & L. Jänsch, (2006) The MprF protein is required for lysinylation of phospholipids in listerial membranes and confers resistance to cationic antimicrobial peptides (CAMPs) on *Listeria monocytogenes*. *Mol Microbiol* **62**: 1325-1339.

Uchiyama, I., T. Higuchi & M. Kawai, (2010) MBGD update 2010: toward a comprehensive resource for exploring microbial genome diversity. *Nucleic Acids Res* **38**: D361-365.

Vences-Guzman, M.A., Z. Guan, J.R. Bermudez-Barrientos, O. Geiger & C. Sohlenkamp, (2013) Agrobacteria lacking ornithine lipids induce more rapid tumour formation. *Environ Microbiol* **15**: 895-906.

Vinuesa, P., F. Neumann-Silkow, C. Pacios-Bras, H.P. Spaink, E. Martinez-Romero & D. Werner, (2003) Genetic analysis of a pH-regulated operon from Rhizobium tropici CIAT899 involved in acid tolerance and nodulation competitiveness. *Molecular plant-microbe interactions : MPMI* **16**: 159-168.

Wallden, K., A. Rivera-Calzada & G. Waksman, (2010) Type IV secretion systems: versatility and diversity in function. *Cell Microbiol* **12**: 1203-1212.

Wessel, M., S. Klüsener, J. Gödeke, C. Fritz, S. Hacker & F. Narberhaus, (2006) Virulence of *Agrobacterium tumefaciens* requires phosphatidylcholine in the bacterial membrane. *Mol Microbiol* **62**: 906-915.

Winans, S.C., (1992) Two-way chemical signaling in *Agrobacterium*-plant interactions. *Microbiol Rev.* **56**: 12-31.

Wirawan, I.G., H.W. Kang & M. Kojima, (1993) Isolation and characterization of a new chromosomal virulence gene of *Agrobacterium tumefaciens*. *J Bacteriol* **175**: 3208-3212.

Wu, H.Y., P.C. Chung, H.W. Shih, S.R. Wen & E.M. Lai, (2008) Secretome analysis uncovers an Hcp-family protein secreted via a type VI secretion system in *Agrobacterium tumefaciens*. *J Bacteriol* **190**: 2841-2850.

Wu, H.Y., K.H. Liu, Y.C. Wang, J.F. Wu, W.L. Chiu, C.Y. Chen, S.H. Wu, J. Sheen & E.M. Lai, (2014) AGROBEST: an efficient Agrobacterium-mediated transient expression method for versatile gene function analyses in Arabidopsis seedlings. *Plant Methods* **10**: 19.

Xie, J., M. Bogdanov, P. Heacock & W. Dowhan, (2006) Phosphatidylethanolamine and monoglucosyldiacylglycerol are interchangeable in supporting topogenesis and function of the polytopic membrane protein lactose permease. *J Biol Chem.* **281**: 19172-19178.

Zhang, Y.M. & C.O. Rock, (2008) Membrane lipid homeostasis in bacteria. *Nat Rev Microbiol* **6**: 222-233.